^{180}Hf energy levels deduced from thermal and average resonance neutron-capture γ-ray spectra

D. L. Bushnell
Northern Illinois University, DeKalb, Illinois 60115
and Argonne National Laboratory, Argonne, Illinois 60439

D. J. Buss
Illinois Benedictine College at Lisle, Lisle, Illinois
and Argonne National Laboratory, Argonne, Illinois 60439

Robert K. Smither
Argonne National Laboratory, Argonne, Illinois 60439
(Received 10 September 1974)

An energy level diagram for ^{180}Hf is developed on the basis of neutron-capture γ-ray spectroscopy. Both thermal neutron capture and average resonance neutron-capture studies were made with isotopically enriched and natural Hf samples. The energies and intensities of the high-energy 7.4–4.7 MeV primary γ transitions and the intermediate-energy 2.1–0.5 MeV γ transitions were made with the in-pile (n,γ) source facility at the Argonne research reactor using Ge(Li) γ-ray detectors. The low-energy 1300–1330 keV γ transitions were measured with the Argonne 7.7 m bent-crystal γ-ray spectrometer which also uses an in-pile (n,γ) source at the Argonne reactor. The final level scheme contains 41 levels with excitation energies up to 2.7 MeV. Twenty-six new levels are reported. Parity assignments are made for all but three of these levels. Unique spin assignments are made for 21 levels and the spin of 15 additional levels was limited to two choices. The possible existence of excited state rotational bands was explored. Two $K=0$ excited state bands and a $K=2$ excited state band were identified.

[NUCLEAR REACTIONS ^{179}Hf(n,γ), measured γ spectrum, E_γ, I_γ, 0.5–2.1 MeV, 4.7–7.4 MeV, Ge(Li) detector, thermal neutrons; measured γ spectrum, E_γ, I_γ, 4.7–7.4 MeV, average resonance neutrons, Ge(Li) detector; measured γ spectrum, E_γ, I_γ, 0.03–1.3 MeV, bent-crystal spectrometer, thermal neutrons. Developed level scheme ^{180}Hf, J^π, γ-ray branching ratios.]

I. INTRODUCTION

As pointed out by Scharff-Goldhaber and McKeown,[1] the level scheme of ^{180}Hf played an important role in the search for evidence of nuclear collective motion in even Z even N nuclei. The discovery of the 5.5 h isomeric state[2] in ^{180}Hf and the subsequent identification[3-11] of the γ rays associated with it as a sequence of $E2$ transitions cascading down through four excited levels with spin 8^+, 6^+, 4^+, and 2^+ to the 0^+ ground state, gave the scientific community its first convincing example of a ground-state rotational band in a deformed even Z even N nucleus. The excitation energy of the levels followed the theoretically predicted $I(I+1)$ dependence so closely that there was no chance of confusing this level scheme with any other description. The relatively long lifetime of the 5.5 h isomeric state with spin 8^- and the corresponding large hindrance factor associated with the $E1$ γ transition to the 8^+ level of the ground-state rotational band provides us with one of the best examples of K forbiddenness ($\Delta K=8$) discovered so far. With this kind of historical background it would seem that the level scheme of ^{180}Hf would be an obvious place to look for additional evidence for collective effects in nuclear structure. In particular one would expect to find additional rotational bands based on new intrinsic states as well as the γ and β bands associated with the ground-state configuration.

An early effort in this direction was made by Smither[12] who used the large bent-crystal diffraction spectrometer[12-15] at Argonne to investigate the low-energy γ-ray spectrum generated by the ^{179}Hf$(n,\gamma)^{180}$Hf reaction. About 100 γ-ray transitions with energies between 80 and 1200 keV were resolved in the work but very little progress was made in developing the level scheme of ^{180}Hf. The energy resolution of the bent-crystal spectrometer was not sufficient to resolve the very complex (n,γ) spectrum above 800 keV so it was not possible

to develop the level scheme above 1 MeV the way a similar study[16] did for ^{178}Hf. The improved energy resolution of the present bent-crystal γ-ray spectrometer system[17] and the use of Ge(Li) detectors has overcome this difficulty to a large degree for the work presented in this paper, but the energy resolution of the 800 to 2000 keV region of the (n,γ) spectrum was still the most difficult part of the data analysis. The main stumbling blocks in the understanding of the ^{180}Hf level scheme were a number of closely spaced doublets and triplets in the level structure which were unresolved in the early work.

The previously published work of Namenson, Jackson, and Smither[18] on the high-energy primary (n,γ) transitions from thermal neutron capture in ^{179}Hf extended the level scheme of ^{180}Hf up to 1610 keV. Many levels were still missed because the resolution of the Ge(Li) detector used was still not sufficient to completely resolve the complex γ-ray spectrum. The recent (d,p) data of Zaitz and Sheline,[19] the Coulomb excitation studies of Varnell, Hamilton, and Robinson,[20] and the β-decay work of Gujrathi and D'Auria[21] and that of Swindle, Ward, and Kuroda[22] have added further information about the level scheme of ^{180}Hf which was quite useful in interpreting the (n,γ) spectrum presented in this paper.

II. EXPERIMENTAL METHODS AND DATA ANALYSIS

Four types of (n,γ) experiments are used in this work to investigate the level scheme of ^{180}Hf. They are:

(1.) Crystal diffraction utilizing the Argonne 7.7 m bent-crystal[12-17] γ-ray diffraction spectrometer to obtain precision energy and intensity measurements on the low-energy, 40 to 1300 keV, portion of the (n,γ) spectrum.

(2.) Ge(Li) γ-ray detectors used in coincidence and anticoincidence with a large split-ring NaI detector[23] to investigate the medium-energy, 400 to 2100 keV, region of the (n,γ) spectrum.

(3.) Ge(Li) detectors used in coincidence with a large (30.5 cm diam) split-ring NaI detector[23] to record the high-energy, 4.7 to 7.3 MeV, portion of the (n,γ) spectrum.

(4.) The average resonance neutron-capture technique[24-26] to measure the energies and averaged intensities of the primary (n,γ) transitions between 5.0 and 7.3 MeV. All experiments made use of enriched and natural samples positioned in the high-flux (3.5×10^{13} n/cm^2 sec) region of the Argonne CP-5 research reactor.

A. Bent-crystal spectrometer measurements

The Argonne 7.7 m bent-crystal γ-ray spectrometer[12-17] was used to investigate the low-energy portion of the (n,γ) spectrum between 40 and 1300 keV. A schematic drawing of the spectrometer is shown in Fig. 1. The neutron-capture γ-ray source was located in the center of a beam tube that passes completely through the central high-flux region of the Argonne CP-5 research reactor. The thermal neutron flux at the source position

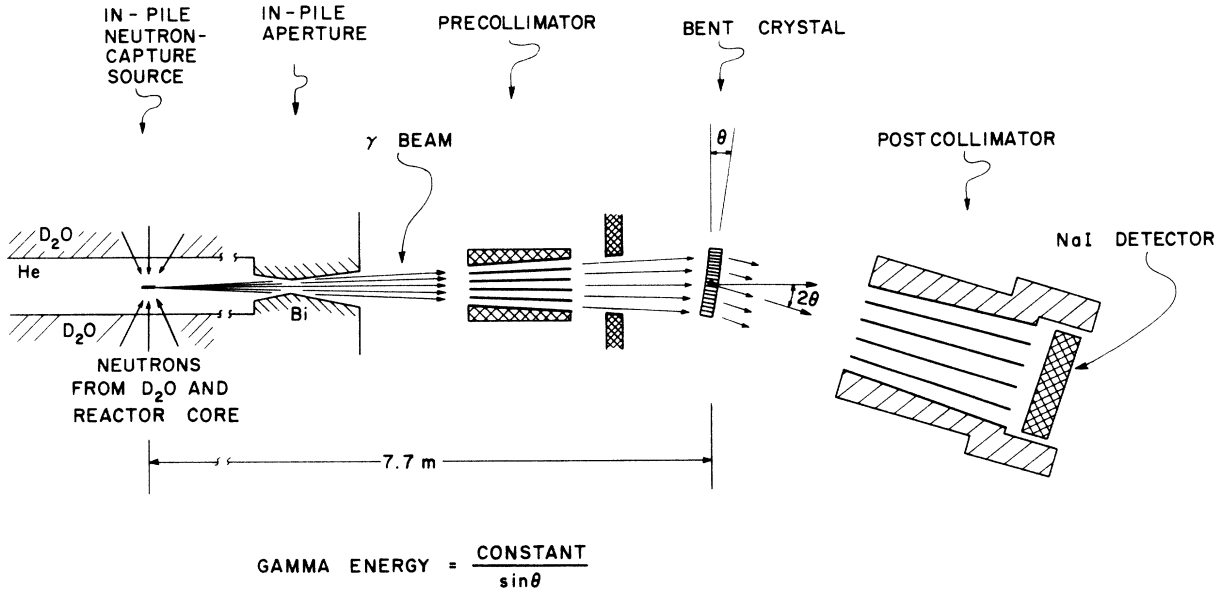

FIG. 1. Schematic drawing of the Argonne 7.7 m bent-crystal γ-ray spectrometrometer.

was 3.5×10^{13} n/cm^2 sec. Three samples with different ^{179}Hf isotropic enrichments were used to identify the γ rays associated with the ^{179}Hf(n,γ)-^{180}Hf reaction. The isotopic enrichment of those samples, along with the contribution of each isotope to the capture rate, is given in Table I. The data from the ^{177}Hf enriched sample have been published in a previous paper by Smither.[16] The enriched ^{179}Hf sample consisted of 324 mg of HfO_2 powder packed in a cavity in a Mg(85%)Al(15%) alloy holder The HfO_2 sample forms a vertical line source 0.018 cm wide and 1 cm deep as viewed from the bent-crystal spectrometer position.

The precision energies and intensities of the 218 low-energy γ-ray transitions seen with the bent-crystal spectrometer are listed in Table II. Unless otherwise noted, the values listed are from the most recent work taken with the 2 mm thick bent-quartz crystal[17] using the 310 diffraction planes. The linewidth of the spectrometer ΔE [full width at half-maximum (FWHM)] is given by $\Delta E(\text{keV}) = 6.0\times E_\gamma^2$ where E_γ is the γ-ray energy in MeV. This gives a linewidth of 60 eV at 100 keV and 6.0 keV at 1 MeV. About one-half of this linewidth is caused by the finite width of the (n,γ) source. Many runs were made over the spectrum. They were analyzed individually at first and then added together and reanalyzed to improve the analysis of the weak lines. When the level scheme development was nearly finished, the γ-ray spectrum was reinvestigated to see if any of the low-energy transitions suggested by the level scheme could be observed when the counting statistics were improved by a factor of 10 or 20. Many of the weak transitions were also reinvestigated to improve their energy and intensity values. This later work causes some variation in the errors quoted for otherwise similar lines in the table. The energy calibration is based on the previously measured values[27] of the K-L_{III} and K-L_{II} Hf x rays, 55.7902 (8) and 54.6114(8), respectively. These values are based on the primary standard, the K-L_{III} x ray of tungsten, which is quoted by Bearden[27] as 59.3182(6) keV.

Most of the problems encountered in the analysis of the data occurred in the energy region above 600 keV. A detailed comparison was made between these bent-crystal data and the Ge(Li) detector data reported in the next section, to make sure that the two analyses were consistent with one another. When information from the Ge(Li) data was used to help analyze the bent-crystal data it is indicated by a footnote. This detailed comparison of the two experiments over the energy region from 500 to 1300 keV made it possible to intercalibrate the energy and intensity values of the medium- and low-energy (n,γ) spectra.

The errors quoted for the γ-ray energies given in Table II are probable errors based on counting statistics, complexity of the spectrum, calibration of the precision screw used to measure the Bragg angle, etc. They do not include any error in the value assumed for the K-L_{III} and K-L_{II} x rays and the measurement of their diffraction angles. The combined uncertainty in this primary calibration is about 1 part in 40 000 and is much smaller than the error quoted for most of the γ rays.

The γ-ray intensities are given in photons per 100 neutron captures and are based on the previously measured efficiency of the bent-crystal spectrometer. The probable error in the intensity is given as a percent of the value given in the table. It includes errors associated with the counting statistics, above mentioned efficiency calibration, complexity of the γ-ray spectrum, uncertainty in the background, etc., but does not include the uncertainty in the neutron-capture cross section[28] and relative isotopic abundance quoted in Table I. The neutron-capture rate for

TABLE I. Information for isotopic identification of γ lines. For a 100% line following neutron capture in a given isotope, the expected intensities in the three targets are equal to the contributions to the total cross section (last three columns). These values, computed from the capture cross section σ and the abundances in the three targets, are given for each stable isotope of hafnium.

Capturing isotope	σ	Composition of target (%)			Contribution to total cross section (%)		
		Natural	Enriched ^{177}Hf	Enriched ^{179}Hf	Natural	Enriched ^{177}Hf	Enriched ^{179}Hf
^{174}Hf	1500 ± 1000	0.18	~0.1(1)	<0.1	2.5	0.42	<2.0
^{176}Hf	15 ± 15	5.15	~0.4(1)	<0.1	0.7	0.02	<0.02
^{177}Hf	380 ± 30	18.39	93.6(2)	1.2(2)	65.0	98.4	7.2
^{178}Hf	75 ± 10	27.08	3.6(1)	4.6(2)	18.9	3.98	5.4
^{179}Hf	65 ± 15	13.78	1.1(1)	83.6(2)	8.3	0.20	85.2
^{180}Hf	14 ± 5	35.44	1.1(1)	10.0(2)	4.6	0.04	2.2

TABLE II. Low-energy γ-ray transitions from the $^{179}Hf(n,\gamma)^{180}Hf$ reaction, as measured with the 7.7 m bent-crystal spectrometer. Both the γ-ray intensity I_γ and the total transition intensity I_{total} represent the number of γ transitions per 100 neutron captures. Entries shown in square brackets are obtained from the Ge(Li) detector spectrum which when appropriately converted to the efficiency and resolution of the bent-crystal spectrum reproduces the bent-crystal envelope very well. A dagger (†) in the "In scheme" column means the γ ray is placed in the level scheme up to 1700.8 keV while a double dagger (‡) means it is placed at an initial state above 1700.8 keV.

E_γ (keV)	In scheme	I_γ (γ's/100 n)	$\Delta I_\gamma/I_\gamma$ (%)	I_{total}	Remarks
45.755 ± 0.007		0.30	20		
53.799 ± 0.001	†	0.32	10	0.93	$E1$
55.448 ± 0.003	†	0.17	25	2.82, 2.77	$E2$, $M1$ may be part of x-ray satellite peak
57.554 ± 0.017	†	0.51	6	1.29	5.5-h isometric transition, $8^- \rightarrow 8^+$
65.24 ± 0.04		0.15	70		
76.623 ± 0.003	†	0.48	10	0.85	
81.21 ± 0.02	†	0.15 [a]	8	1.23, 1.26	$E2$, $M1$
92.44 ± 0.01 [a]	†	0.014 [a]	55	0.09	$E2$
92.50 ± 0.01 [a]		0.015 [a]	51		
92.56 ± 0.01 [a]		0.016 [a]	47		
92.797 ± 0.008 [a]		0.06 [a]	14		
93.324 ± 0.002	†	9.85	1	60.7	$2^+ \rightarrow 0^+$, g.s. band
96.589 ± 0.01 [a]	†	0.017 [a]	32	0.10	$E2$
104.604 ± 0.01 [a]		0.0084 [a]	55		
104.692 ± 0.01 [a]		0.0080 [a]	57		
105.433 ± 0.01 [a]		0.039 [a]	15		
108.308 ± 0.002	†	1.90	4	6.9, 8.6	$E2$, $M1$
109.474 ± 0.003	†	0.62	9	2.2, 2.8	$E2$, $M1$
113.66 ± 0.02 [a]	†	0.05 [a]	18	0.09	$E1$
113.71 ± 0.01 [a]		0.13 [a]	7		
115.91 ± 0.02		0.14 [b]	(15)		
123.93 ± 0.003		0.54	10		
(125.26 ± 0.03)	†	0.07	50		No certain isotopic assignment
130.260 ± 0.003		0.65	9		
135.09 ± 0.01		0.48	10		
138.05 ± 0.03		0.08	46		
141.55 ± 0.01	†	0.17	22	0.35, 0.43	$E2$, $M1$
152.05 ± 0.03 [c]		0.135 [c]	(8)		
155.06 ± 0.06 [c]		0.05 [c]	(15)		
155.60 ± 0.06 [c]		0.03 [c]	(18)		
158.33 ± 0.06		0.03	67		
160.40 ± 0.03		0.12	27		
161.67 ± 0.08		0.04	80		
163.07 ± 0.04		0.05	80		0.05% ^{178}Hf has been removed
163.41 ± 0.02		0.11	35		
167.10 ± 0.01		0.30	12		
168.80 ± 0.05 [c]	†	0.06 [c]	(14)		
177.71 ± 0.03	†	0.17	20	0.25, 0.31	$E2$, $M1$
177.86 ± 0.03	†	0.19	20	0.20	$E1$
181.26 ± 0.04	†	0.06	54		
185.25 ± 0.04		0.06	54		
186.04 ± 0.02		0.19	18		
188.14 ± 0.02	†	0.17	20		
192.83 ± 0.02		0.24	15		
198.35 ± 0.07	†	0.04	84		
203.27 ± 0.08		0.07	48		No certain isotopic assignment
205.51 ± 0.01		1.35	3.9		
207.98 ± 0.02		0.59	7.2		
209.51 ± 0.07	†	0.04	84		
215.252 ± 0.002	†	34.5	0.6	41.7	$4^+ \rightarrow 2^+$, g.s. band

TABLE II *(Continued)*

E_γ (keV)	In scheme	I_γ (γ's/100 n)	$\Delta I_\gamma / I_\gamma$ (%)	I_{total}	Remarks
219.7 ±0.1 [c]		0.04 [c]	(20)		
223.76 ±0.06	†	0.06	64		
233.33 ±0.08	†	0.22	23		
235.020 ±0.006	†	4.46	2.5		
238.56 ±0.05	†	0.79	8.0		
243.40 ±0.10	†	0.10	51		
254.61 ±0.09 [a]	†	0.19 [a]	7		
255.34 ±0.03 [a]	†	0.08 [a]	16		
(258.21 ±0.06) [a]		0.045 [a]	23		On wing of strong 178→179 line
258.90 ±0.03 [a]	†‡	0.10 [a]	12		
260.08 ±0.03 [a]		0.08 [a]	15		
261.18 ±0.03 [a]		0.13 [a]	9		
265.27 ±0.06 [a]		0.06 [a]	21		
266.07 ±0.02 [a]		0.19 [a]	7		
274.6 ±0.10 [c]	†	0.16 [b]	10		
282.28 ±0.08	†	0.42	15		
284.60 ±0.10 [c]		0.23 [c]	30		
291.01 ±0.08 [c]		0.32 [c]	23		
302.06 ±0.08	†	0.23	30		
306.4 ±0.10 [c]	†	0.15 [c]	10		
310.4 ±0.10 [c]		0.06 [c]	15		
313.5 ±0.10 [c]	†	0.13 [c]	10		^{178}Hf contribution undetermined
319.25 ±		0.06			
316.61 ±0.06	†	0.64	13		$6^+ \rightarrow 4^+$, g.s. band
332.271 ±0.010 [a]	†	9.25	2.2		
344.1 ±0.10 [c]		0.06 [c]	15		
346.25 ±0.14	†	0.37	25		
355.2 ±0.10 [c]	†	0.10 [c]	30		
358.2 ±0.10 [c]		0.03 [c]	50		
363.32 ±0.10		0.16	21		
365.58 ±0.03		0.28	11		
367.36 ±0.07		0.17	20		
385.84 ±0.14	†	0.19	20		
388.45 ±0.14	†	0.25	16		Possible ^{178}Hf line in this doublet
389.95 ±0.07		0.39	7		
391.06 ±0.13		0.13	22		No certain isotopic assignment
392.38 ±0.38		0.14	21		
407.94 ±0.02 [a]	†	1.57	2		May contain weak ^{178}Hf line at 408.3 keV
409.61 ±0.08 [a]	†	0.18	15		
410.5 ±0.1		0.06	40		
420.96 ±0.10 [a]		0.33 [a]	8		
433.71 ±0.12 [a]		0.34 [a]	8		
440.87 ±0.20 [a]		0.20 [a]	13		
443.09 ±0.04 [d]	†	1.69	2		$8^+ \rightarrow 6^+$, g.s. band
446.87 ±0.05 [a]		0.56 [a]	5		
451.64 ±0.08 [a]		0.35 [a]	6		
452.53 ±0.16 [a]	‡	0.16 [a]	20		
465.25 ±0.11		0.35	9		
476.86 ±0.07		0.57	6		
487.29 ±0.08		0.55	7		
500.64 ±0.18	†	0.18	21		
527.08 ±0.03 [a]		0.73	5		
530.10 ±0.08 [a]		0.24	20		
534.52 ±0.04 [a]		0.60	7		
538.39 ±0.04 [a]	‡	0.65	6		

TABLE II *(Continued)*

E_γ (keV)		In scheme	I_γ (γ's/100 n)	$\Delta I_\gamma / I_\gamma$ (%)	I_{total}	Remarks
551.75	±0.06 [a]	†‡	0.24	15		
577.56	±0.08 [a]		0.14	25		
[583.4	±0.5		0.13	60]		
[585.0	±0.5		0.15	60]		Broadened Mg line from target holder
[586.9	±0.6		0.14	60]		covers these lines in the bcs spectrum
[588.6	±0.5		0.13	60]		
595.6	±0.5		0.07	80		Probably due to ^{180}Hf
621.3	±0.4		0.41	15		
644.3	±0.6		0.28	60		May have some ^{178}Hf intensity
654.9	±0.6	‡	0.13	15		Has some ^{179}Hf intensity
659.1	±0.5		0.26	50		
664.1	±0.6		0.18	50		
[667.9	±0.4		0.17	40]		
[680.1	±0.5		0.09	50]		
[681.8	±0.5		0.10	50]		
[683.7	±0.4		0.12	50]		
[686.9	±0.3		0.14	40]		
[690.1	±0.6		0.12	60]		
[691.4	±0.5		0.13	40]		
[703.3	±0.5	‡	0.11	50]		
[707.3	±0.5	‡	0.09	50]		
[709.8	±0.4	‡	0.10	50]		
[714.6	±0.3		0.10	60]		
[716.1	±0.3		0.16	40]		
[725.6	±0.2		0.42	15]		Triplet envelope agrees with sum
[728.1	±0.3		0.27	30]		of lines from Ge(Li)
[729.9	±0.3		0.28	30]		spectrum
[741.9	±0.4		0.14	50]		bcs triplet centroid
[743.4	±0.2	‡	0.30	20]		at 743.5 ± 0.8 keV
[745.4	±0.4		0.14	40]		and $I = 0.40$
[758.1	±0.4		0.20	40]		
[761.1	±0.3		0.09	50]		
[763.3	±0.5		0.11	40]		
[764.8	±0.5		0.13	35]		
[768.1	±0.6		0.12	30]		
[779.3	±0.5		0.10	40]		
[784.5	±0.5		0.08	60]		
[786.1	±0.5		0.10	50]		
[787.6	±0.5		0.14	35]		
[792.1	±0.5		0.11	50]		
[794.0	±0.5		0.10	50]		
799.9	±0.3 [e]		0.38 [a]	20		
[803.6	±0.7		0.09	50]		
[809.9	±0.3		0.20	20]		
[811.8	±0.7		0.07	70]		
[819.7	±0.6		0.10	50]		
[830.8	±0.4		0.18	25]		
[844.8	±0.7		0.07	90]		bcs triplet centroid
[846.2	±0.6		0.15	30]		at 846.8 [e] ± 0.9
[847.3	±0.7		0.06	90]		and $I = 0.20$
[853.8	±0.5		0.09	60]		
[856.2	±0.5		0.09	60]		

TABLE II *(Continued)*

E_γ (keV)	In scheme	I_γ (γ's/100 n)	$\Delta I_\gamma / I_\gamma$ (%)	I_{total}	Remarks
[857.5 ±0.5		0.11	60]		
[864.2 ±0.3		0.14	30]		
[880.8 ±0.7		0.12	50]		
[884.7 ±0.7		0.10	70]		
[890.2 ±0.5		0.21	40]		
[892.4 ±0.5		0.20	40]		
[913.8 ±0.5		0.09	80]		bcs quadruplet centroid at 916.5 [e]
[915.8 ±0.4		0.49	15]		
[917.4 ±0.5		0.25	30]		Summed Ge(Li) lines reproduce bcs envelope
[921.0 ±0.5		0.14	25]		
[928.4 ±0.5		0.13	50]		
[930.8 ±0.5		0.13	50]		
[935.4 ±0.5		0.14	70]		
[938.8 ±0.5		0.20	50]		
[946.6 ±0.6		0.15	60]		
[956.3 ±0.5		0.16	50]		
[965.8 ±0.5		0.14	50]		
[968.8 ±0.4		0.40	20]		
[973.0 ±0.5		0.18	25]		
[977.9 ±0.7		0.12	40]		
[979.7 ±0.7		0.11	80]		
982.0 ±0.5 [e]		0.94	5		
1003.0 ±0.4 [e]		0.54	10		
[1011.7 ±0.4		0.13	30]		
[1017.1 ±0.1		1.0	6]		
[1019.3 ±0.5 [d]		0.11	70]		
[1022.9 ±0.5		0.16	35]		
[1030.5 ±1.0		0.07	100]		
[1034.9 ±0.5		0.10	70]		
[1041.7 ±0.5		0.13	40]		
[1054.6 ±0.4		0.28	25]		
[1061.0 ±0.3		2.65	5]		
1065.60 ±0.06		26.8	1		Doublet centroid [g]
[1071.1 ±0.5		0.41	40]		
[1077.4 ±0.2		0.30	50]		
[1083.2 ±0.4		0.44	40]		
[1085.6 ±0.5		0.08	80]		
[1097.6 ±0.7		0.14	60]		
[1100.6 ±0.15		2.43	5]		bcs triplet centroid at 1103.4 keV members: 1100.6(2.43), 1103.1(0.890) ^{178}Hf, and 1106.0(2.48) obtained from Ge(Li) data which sum correctly to bcs envelope [h]
[1106.0 ±0.15		2.48	5]		
[1110.5 ±0.6		0.13	40]		
[1117.0 ±0.6		0.12	30]		
[1121.7 ±0.5		0.36	16]		
[1123.0 ±1.0		0.05	70]		
[1127.6 ±0.8		0.08	70]		
[1138.4 ±1.0		0.12	40]		
[1140.8 ±0.8		0.21	30]		
[1151.7 ±0.5		0.28	16]		
[1163.9 ±1.0		0.13	50]		
[1181.8 ±1.0		0.10	70]		

TABLE II *(Continued)*

E_γ (keV)		In scheme	I_γ (γ's/100 n)	$\Delta I_\gamma / I_\gamma$ (%)	I_{total}	Remarks
[1185.8	±0.6		0.12	50]		
1197.8	±0.2		7.0	5]		bcs doublet [containing 1197.8 keV(4.3%) and 1199.7 keV(2.8%)][h]
[1206.9	±0.3		1.6	15]		
[1211.9	±0.6		0.15	40]		
[1226.5	±0.5		0.20	30]		
[1231.9	±0.5		0.34	20]		
1248.8	±0.3 [d]		2.9	3		Unresolved from 1260.9 keV line [i]
1260.9	±0.12 [d]		4.8	4		Unresolved from 1248.8 keV line [i]

[a] Obtained from bent-crystal spectrometer (bcs) runs where especially long counting times were obtained by running over the peak many times in what is called the "autocycle model."

[h] Intensity normalized to bcs data.

[c] Energy obtained from measurements taken with the bent-crystal spectrometer using three targets of differing abundances for isotopic identification.

[d] From special bcs "autocycle" calibration runs.

[e] High energy bcs data compared to Ge(Li) data for assistance in understanding multiplets.

[f] Intensity obtained from Ge(Li) spectrometer data.

[g] The Ge(Li) data resolves the members of this doublet and provides an intensity ratio for unfolding the members in the bcs data. This calibrates the energy of the strong member.

[h] See Ge(Li) data for resolution of this multiplet.

[i] The intensity ratio established here is used in the Ge(Li) data where a carbon line blends with the doublet to form a triplet.

^{179}Hf should include a contribution from the capture of resonance neutrons which may be as much as 5% of the thermal capture rate because the sample is exposed to the full reactor neutron flux. When the error in the neutron-capture cross section (20 %) becomes smaller, this will have to be taken into account in recalculating the absolute intensities.

Figures 2 and 3 depict the γ-ray spectrum observed below 800 keV. Some of the weaker transitions do not show, but the high degree of complexity is obvious in the 100 to 300 keV region and again in the region above 600 keV. The energy resolution of the spectrometer was usually sufficient to resolve the spectrum in the low-energy region (see example of data near the 93 keV transition shown in Fig. 4), but the region above 600 keV needs an instrument with at least a factor of 4 improvement in its energy resolution to do a good job analyzing the spectrum.

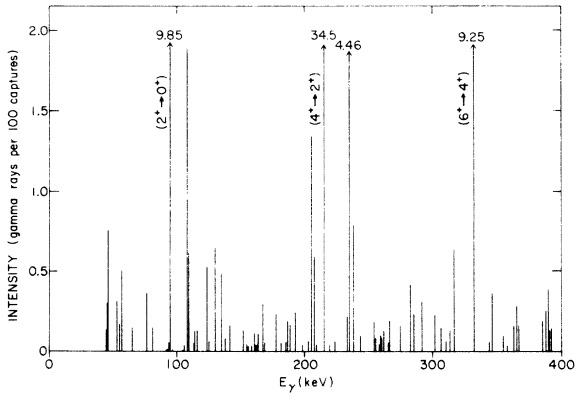

FIG. 2. A line drawing description of the ^{179}Hf(n, γ)^{180}Hf spectrum in the range 0–400 keV.

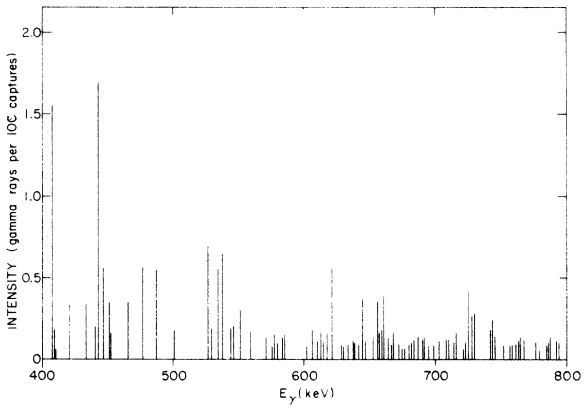

FIG. 3. A line drawing description of the ^{179}Hf(n, γ)^{180}Hf spectrum in the range 400–800 keV.

B. Ge(Li) detector γ-ray spectrum from 500 to 2200 keV

The portion of the (n,γ) spectrum between 500 and 2200 keV was investigated with a Ge(Li) γ detector located inside a NaI annular-ring detector.[23] This medium-energy spectrum was recorded in the anticoincidence mode so that no pulses were stored in the multichannel analyzer when an event occurred in the surrounding NaI ring. This method strongly enhances the full energy peaks over the partial energy loss events. Figures 5 and 6 show the ^{179}Hf$(n,\gamma)^{180}$Hf γ-ray spectrum between 800 and 2000 keV. The measured energies and intensities are listed in Table III. The format is the same as in Table II. Intensities are given in photons per 100 neutron captures in ^{179}Hf. The isotopic enrichment of the ^{179}Hf sample was the same as that used in the bent-crystal spectrometer work (see Table I). Again the isotopic assignments are based on the comparison of the relative intensities obtained with samples containing three different enrichments of ^{179}Hf (see Table I).

The energy and intensity calibration of the medium-energy (n,γ) spectrum is based on the bent-crystal spectrometer data for the strong lines in this energy range. The two spectra are normalized so that they agree exactly in both energy and intensity for the 1065.77 keV doublet. This doublet energy region is shown in detail in Fig. 7. Above 900 keV the energy resolution of the Ge(Li) detector was appreciably better than that of the bent-crystal spectrometer. In this energy region and above, the Ge(Li) detector data were analyzed first to obtain the energy spacings and relative intensities of the separate components of a complex peak structure. This information was then used to generate the expected response function for the bent-crystal spectrometer. The whole structure was then fitted as a unit to the bent-crystal data. Using this technique it was possible to obtain more accurate values for energies and intensities of the γ lines than could be obtained with either the Ge(Li) detector or the bent-crystal spectrometer used alone. This

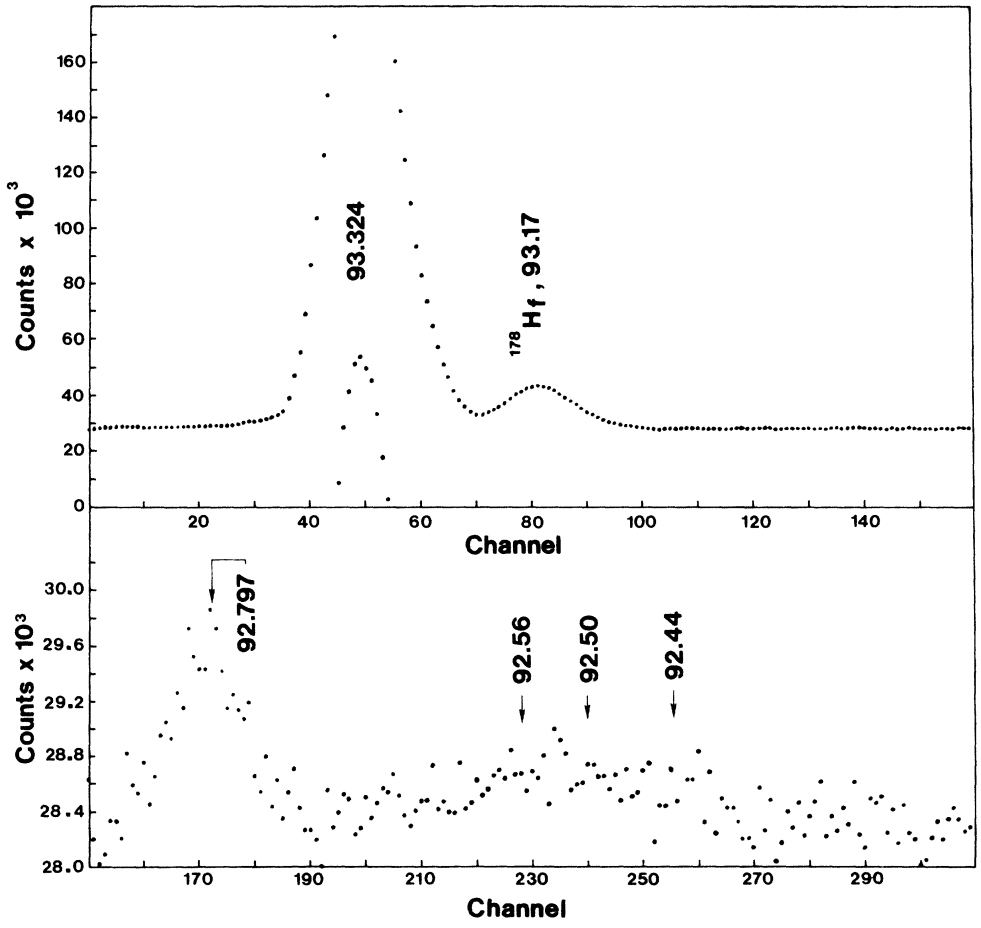

FIG. 4. Portion of ^{179}Hf$(n,\gamma)^{180}$Hf spectrum near the 93.324 keV transition.

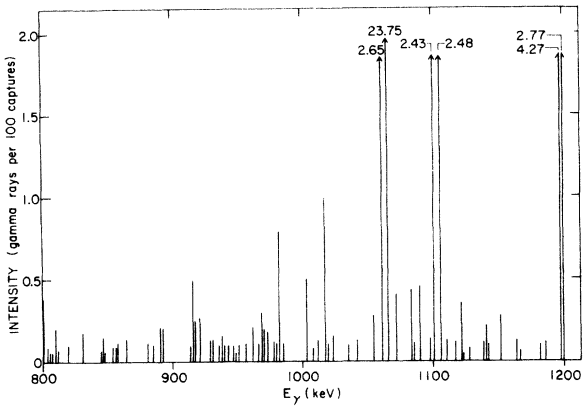

FIG. 5. A line drawing description of the $^{179}Hf(n, \gamma)^{180}Hf$ spectrum from 800 to 1200 keV.

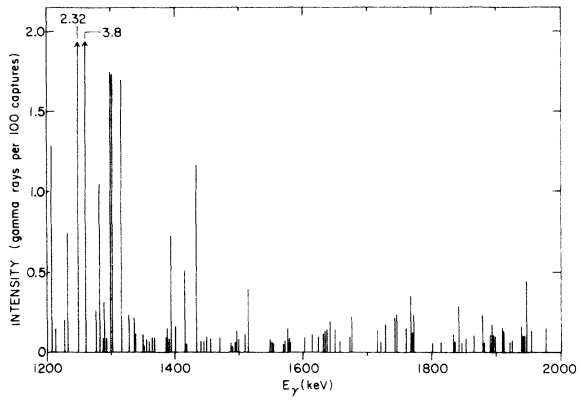

FIG. 6. A line drawing description of the $^{179}Hf(n, \gamma)^{180}Hf$ spectrum from 1200 to 2000 keV.

method was used to extend the energy and intensity calibration up to 1300 keV. Above 1300 keV the energy and intensity values are based on previous calibrations of the linearity of the multichannel analyzer and the relative efficiency of the Ge(Li) detector system. Figure 8 shows the raw data for one of the six Ge(Li) detector runs made in this energy region.

The Ge(Li) detector system was subject to line broadening if a high count rate were used. The data shown in Fig. 8 were taken with an appreciable amount of absorbing material in the beam (30.5 cm of borated polyethelene and 1.55 cm of thorium) to reduce this line broadening effect. The use of these absorbers results in a reduction in the sensitivity of the experiment for low-energy γ rays. This low-energy absorption is noticeable in Fig. 8 below 900 keV and becomes quite large below 600 keV. It is for this reason that Table III does not go below 500 keV.

C. Thermal neutron-capture Ge(Li) detector data for $E_\gamma = 4.7$ to 7.3 MeV

The thermal neutron-capture γ-ray spectrum for γ energies between 4.7 and 7.3 MeV was re-

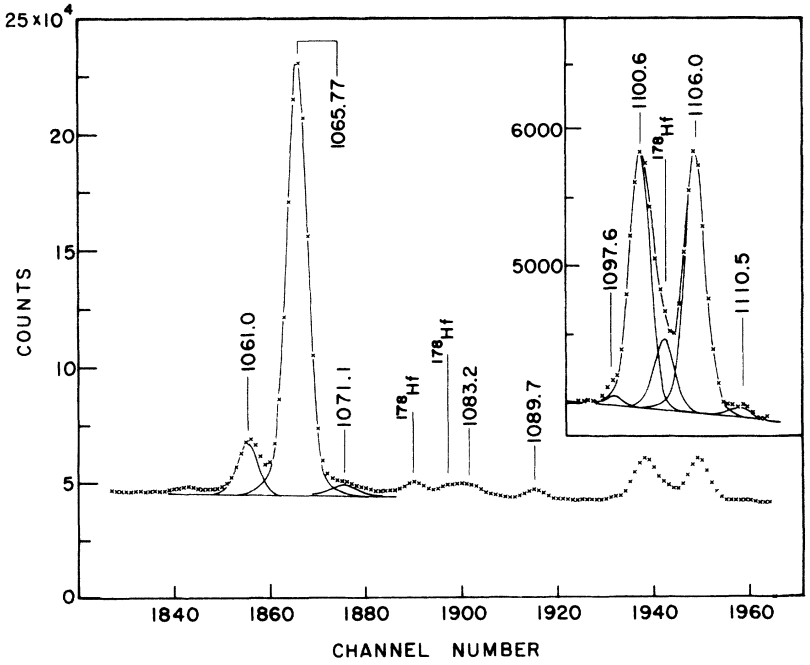

FIG. 7. Portion of the $^{179}Hf(n, \gamma)^{180}Hf$ spectrum near the 1065.77 keV doublet.

TABLE III. Medium energy γ rays from the ^{179}Hf$(n,\gamma)^{180}$Hf reaction as measured with a Ge(Li) detector. Target abundances are 1.2% and 83.6% for ^{177}Hf and ^{179}Hf, respectively. I_γ is given in transitions per 100 neutron captures. A dagger (†) in the "In scheme" column indicates that the γ ray has been placed in the 0–1700 keV range of the partial level scheme while a double dagger (‡) indicates that the γ ray has been placed in the range of the level scheme above 1700 keV.

E_γ (keV)	In scheme	I_γ	$\Delta I_\gamma / I_\gamma$ (%)	Remarks
526.9 ±0.2		0.70	25	
529.6 ±0.4		0.22	40	Possible contribution from ^{181}Hf and ^{179}Hf
534.4 ±0.2		0.26	40	Unfolded from ^{178}Hf at 534.3 keV [I_{total} = 0.56 ± (20)]
538.0 ±0.2		0.65	15	
551.4 ±0.3	†‡	0.30	30	
577.0 ±0.3		0.15	40	Probably ^{180}Hf
583.4 ±0.5		0.13	60	Complicated multiplet structure located on uncertain background. There are traces of ^{178}Hf lines at 584.2 keV and 588.5 keV.
585.0 ±0.5		0.15	60	
586.9 ±0.6		0.14	66	
588.6 ±0.5		0.09	60	The ^{178}Hf contribution has been removed (Total I = 0.13%).
617.7 ±0.6		0.17	50	^{178}Hf contribution <0.06
621.2 ±0.3		0.56	10	
644.5 ±0.3		0.33	25 [a]	
646.6 ±0.6		0.06	60 [a]	Unfolded from ^{178}Hf (Total I = 0.10)
654.9 ±0.3	‡	0.13	30 [a]	Has some ^{179}Hf at 654.9 keV.
657.1 ±0.7		0.09	60 [a]	^{178}Hf contribution removed (total intensity = 0.14 at 657.0 keV)
659.1 ±0.7		0.18	60 [a]	
664.1 ±0.7		0.13	50 [a]	
667.9 ±0.4		0.17	40 [a]	Possible ^{178}Hf contribution
680.1 ±0.5		0.09	55	Uncertain identification
681.8 ±0.5		0.10	50	Uncertain identification, possible Hf mixture
683.7 ±0.4		0.12	50	Uncertain identification, possible Hf mixture
686.9 ±0.3		0.14	35	Uncertain identification, possible Hf mixture
690.1 ±0.6		0.12	60	Uncertain identification
691.4 ±0.5		0.13	40	
703.3 ±0.5	‡	0.11	50	Uncertain identification, possible Hf mixture
707.3 ±0.5	‡	0.09	50	Uncertain identification
709.8 ±0.4	‡	0.16	50	
714.6 ±0.3		0.10	60	Uncertain identification, both 178 and 180 possible
716.1 ±0.3		0.16	40	Uncertain identification, both 178 and 180 possible
725.6 ±0.2		0.42	13	
728.1 ±0.5	†	0.23	28	Probably ^{180}Hf
729.9 ±0.3		0.28	27	Probably ^{180}Hf
741.9 ±0.4		0.14	40	<16% of I due to ^{178}Hf
743.4 ±0.2	†	0.24	20	Probably ^{180}Hf
745.4 ±0.4		0.14	40	≤30% of I due to ^{178}Hf
758.1 ±0.4		0.15	40	
761.1 ±0.3		0.08	50	
763.3 ±0.5		0.11	40	Probably ^{180}Hf
764.8 ±0.5		0.13	35	Possible ^{180}Hf
768.1 ±0.6	†	0.12	30	0.06 to ^{180}Hf and 0.06 to ^{178}Hf
779.3 ±0.5		0.10	40	
784.5 ±0.5		0.08	60	
786.1 ±0.5		0.10	50	Probably ^{180}Hf
787.8 ±0.5		0.14	35	Probably ^{180}Hf
792.1 ±0.5		0.11	45	
794.0 ±0.5		0.10	50	Possible ^{180}Hf
800.3 ±0.15		0.38	11	
803.6 ±0.7		0.09	55	Possible ^{180}Hf
809.9 ±0.3		0.20	20	

TABLE III *(Continued)*

E_γ (keV)	In scheme	I_γ	$\Delta I_\gamma / I_\gamma$ (%)	Remarks
811.8 ± 0.7		0.07	70	Possible ^{180}Hf
819.7 ± 0.6		0.10	50	Possible doublet
830.8 ± 0.6	†	0.18	25	Located on the Compton edge of 1066 keV line
844.8 ± 0.7		0.07	90	Located on the Compton edge of 1066 keV line
846.2 ± 0.6		0.15	30	Located on the Compton edge of 1066 keV line
847.3 ± 0.7		0.06	90	Located on the Compton edge of 1066 keV line
853.8 ± 0.5		0.09	60	Located on the Compton edge of 1066 keV line
856.2 ± 0.5		0.09	65	Located on the Compton edge of 1066 keV line
857.5 ± 0.5		0.11	65	Located on the Compton edge of 1066 keV line
864.2 ± 0.3		0.14	30	Located on the Compton edge of 1066 keV line
880.8 ± 0.7		0.12	50	
884.7 ± 0.7	†	0.10	70	Possible ^{180}Hf
888.5 ± 0.7		0.08	80	
890.9 ± 0.4		0.28	20	
893.4 ± 0.7		0.10	60	
913.8 ± 0.8		0.09	80	Possible ^{180}Hf
915.8 ± 0.3		0.49	15	Triplet structure
917.4 ± 0.5		0.25	30	
921.0 ± 0.3		0.14	25	Probably ^{180}Hf
928.4 ± 0.5		0.13	50	Doublet or triplet
930.8 ± 0.5		0.13	50	
935.4 ± 0.5		0.19	65	Triplet structure with 939.1 keV ^{178}Hf γ ray
937.8 ± 0.5		0.16	50	
946.6 ± 0.6		0.10	60	Possible ^{180}Hf
950.6 ± 0.5		0.11		
952.2 ± 0.7	†	0.05		
956.3 ± 0.5	†	0.11	50	Possible ^{180}Hf
965.8 ± 0.5		0.11	50	
968.8 ± 0.4		0.40	19	
973.0 ± 0.5		0.18	25	
977.9 ± 0.7		0.12	40	
979.7 ± 0.7		0.11	100	
982.1 ± 0.3	†	0.85	6	
1003.2 ± 0.5		0.51	15	
1011.7 ± 0.5		0.13	30	
1014.3 ± 0.6	†	0.10	80	
1017.1 ± 0.1		0.99	6	
1019.3 ± 0.5		0.11	70	Possible ^{180}Hf
1022.9 ± 0.5		0.16	35	
1030.4 ± 0.6		0.07	80	Possible ^{180}Hf (~0.04 of the 0.07 can be assigned to ^{178}Hf)
1034.9 ± 0.5		0.10	70	
1039.7 ± 0.6		0.08	70	Possible ^{180}Hf (~0.02 of the 0.08 can be assigned to ^{178}Hf)
1041.7 ± 0.5		0.13	40	
1046.1 ± 0.6		0.09	70	Possible ^{180}Hf (~0.04 of the 0.09 can be assigned to ^{178}Hf)
1054.6 ± 0.4		0.28	25	May be doublet
1061.0 ± 0.3	††	2.65	5	
1065.77 ± 0.05	†	23.75	1	Calibration line: Intensity from bcs: The total energy error is ± 0.08 combining the bcs calibration error of 0.06 and the Ge(Li) random error of ± 0.05.
1070.7 ± 0.5		0.36	40	In the wing of 1066 keV line
1072.6 ± 0.5		0.14	70	Subtracted from a close doublet with a ^{178}Hf line
1077.4 ± 0.2		0.30	50	

TABLE III *(Continued)*

E_γ (keV)	In scheme	I_γ	$\Delta I_\gamma / I_\gamma$ (%)	Remarks
1083.2 ±0.4	‡	0.44	40	Unfolded from quadruplet
1085.6 ±0.5		0.08	65	including 1080.8 from ^{178}Hf
1097.6 ±0.7		0.14	60	
1100.6 ±0.15	†	2.43	5	Lines unfolded from a triplet with a ^{178}Hf line at
1106.0 ±0.15	†	2.48	5	1103.1 keV (0.8%)
1110.5 ±0.6		0.13	40	
1117.0 ±0.6		0.12	30	
1121.7 ±0.5	†	0.36	16	
1123.0 ±1.0		0.05	100	Possible ^{180}Hf line
1127.6 ±0.8		0.08	70	Possible ^{180}Hf line
1138.4 ±1.0		0.12	40	
1140.8 ±0.8		0.21	30	
1151.7 ±0.5		0.28	16	
1163.9 ±1.0	†	0.13	50	Some chlorine contamination possible
1167.0 ±1.0		0.07	100	This line lies under ^{178}Hf (I_γ = 0.71, E_γ = 1166.7 keV)
1181.8 ±1.0		0.10	70	
1185.8 ±0.6		0.12	50	
1197.8 ±0.3	†	4.27	7	
1199.7 ±0.4	†	2.77	10	
1206.9 ±0.3	†	1.60	15	^{178}Hf contribution of 1.20 has been removed
1211.9 ±0.6		0.15	40	
1231.9 ±0.5 [b]	†	0.74	10	(Unknown amount of impurity)
1249.1 ±0.1		2.32	3	
1260.8 ±0.3	†	3.8 [c]	12	Doublet with ^{13}C line (1261.9 keV), centroid = 1261.5 ± 0.2 keV
1276.5 ±0.4	†	0.27	20	Probable ^{180}Hf line
1281.7 ±0.2	†	1.05	5	
1286.9 ±1.0		0.09	70	Possible ^{180}Hf line
1288.7 ±0.5	†	0.32	25	
1299.0 ±0.6		0.5	6	
1300.5 ±0.4	†	1.85	6	
1302.0 ±0.5		1.10	6	
1316.4 ±0.3	†	1.70	3	
1328.4 ±1.0	†	0.23	20	
1336.8 ±1.0	†	0.22	40	
1338.3 ±1.0		0.12	90	
1350.7 ±0.5		0.11	20	
1352.2 ±0.8		0.04	90	Uncertain identification
1359.4 ±1.0		0.07	70	Possible ^{180}Hf line
1367.1 ±1.0		0.09	70	
1386.5 ±1.0		0.09	80	
1389.0 ±0.7	†	0.15	40	
1391.1 ±1.0	††	0.08	90	
1394.5 ±0.3		0.72	7	
1400.5 ±0.5	‡	0.16	40	25% of the 0.16 may be due to ^{178}Hf
1416.7 ±0.3	‡	0.51	11	
1440.5 ±0.0		0.07	80	50% of the intensity may be due to ^{178}Hf
1446.9 ±1.0	†	0.07	80	50% of the intensity may be due to ^{178}Hf
1449.5 ±0.7		0.10	60	
1456.4 ±1.0		0.08	60	
1469.6 ±0.7		0.09	60	Possible ^{180}Hf line
1488.0 ±1.0		0.06	90	
1490.7 ±1.0		0.04	100	
1493.9 ±1.0		0.06	90	
1499.9 ±1.0		0.08	80	
1503.3 ±0.6		0.08	80	

TABLE III *(Continued)*

E_γ (keV)	In scheme	I_γ	$\Delta I_\gamma / I_\gamma$ (%)	Remarks
1510.5 ± 0.7		0.11	50	
1515.4 ± 0.4	†	0.27	15	
1516.5 ± 0.4	†	0.21	30	
1543.8 ± 0.5	†	0.10	50	
1550.2 ± 0.7		0.08	70	
1552.2 ± 0.7		0.07	80	
1553.8 ± 1.0		0.06	90	
1570.3 ± 1.0		0.05	90	
1572.0 ± 1.0		0.07	80	
1577.0 ± 0.4		0.15	40	
1578.7 ± 0.7		0.08	80	
1580.8 ± 1.0		0.06	90	
1603.0 ± 0.4		0.09	60	
1614.7 ± 0.4		0.11	45	
1623.9 ± 0.4		0.10	50	Has some ^{178}Hf included (~20% of the listed intensity)
1631.4 ± 0.7	†	0.12	40	
1633.8 ± 0.7		0.13	40	
1636.8 ± 0.5	†‡	0.14	40	
1642.2 ± 0.5		0.19	40	
1650.2 ± 0.7	‡	0.14	50	
1657.7 ± 0.5		0.07	80	
1672.8 ± 0.7		0.09	80	
1675.6 ± 0.4		0.22	40	
1715.6 ± 0.7		0.14	50	
1721.0 ± 0.7	‡	0.07	80	
1727.8 ± 0.2		0.17	40	
1743.2 ± 0.2	‡	0.21	30	Has some ^{178}Hf included (~30% of listed intensity)
1746.3 ± 0.3		0.23	30	
1759.9 ± 0.4		0.15	50	
1767.6 ± 0.2		0.35	25	
1769.8 ± 0.5		0.12	60	Triplet
1771.8 ± 0.3		0.23	40	
1800.8 ± 1.0		0.06	80	No certain isotopic assignments
1813.8 ± 1.0		0.06	80	No certain isotopic assignments
1833.9 ± 0.7		0.11	40	
1835.8 ± 1.0		0.07	80	No certain isotopic assignments
1841.5 ± 0.3		0.28	25	
1853.0 ± 0.7		0.08	80	No certain isotopic assignments
1864.8 ± 0.5		0.10	60	
1879.0 ± 0.2		0.23	30	
1881.3 ± 0.8		0.06	100	No certain isotopic assignments
1890.0 ± 0.7		0.10	60	Probably primarily ^{180}Hf
1892.5 ± 0.5		0.17	40	About equally due to ^{178}Hf and ^{180}Hf
1895.5 ± 0.7		0.10	60	
1898.2 ± 1.0		0.09	70	About equally due to ^{178}Hf and ^{180}Hf
1909.0 ± 0.7		0.15	40	
1911.4 ± 0.7		0.13	50	
1920.9 ± 1.0		0.06	90	
1923.8 ± 1.0		0.07	80	
1938.5 ± 0.5		0.16	40	
1941.0 ± 0.7	‡	0.10	60	
1942.9 ± 0.7		0.10	60	
1946.5 ± 0.7	‡	0.44	12	
1954.8 ± 0.7		0.13	60	
1977.7 ± 1.6		0.14	40	

TABLE III *(Continued)*

E_γ (keV)	In scheme	I_γ	$\Delta I_\gamma / I_\gamma$ (%)	Remarks
2008.3 ±1.7	‡	0.15	40	
2051.7 ±1.7		0.10	60	
2058.3 ±1.7		0.10	60	
2085.1 ±1.7		0.09	80	
2089.1 ±1.0		0.10	80	
2106.4 ±1.7		0.14	40	
2118.7 ±1.9		0.15	40	
2160.0 ±1.9		0.14	40	
2183.5 ±1.9		0.89	8	
2199.2 ±1.8		0.17	30	
2238.5 ±1.8		0.08	80	

[a] Intensity errors are extra large due to special background uncertainties.

[b] In the ^{177}Hf$(n,\gamma)^{178}$Hf experiment, both of these lines are weaker and unresolved from a much stronger 1229 keV line coming from ^{178}Hf. Since no line from ^{180}Hf can appear in that run, their origin in this experiment is unknown. The ratio of the 1229 keV line intensity in the two experiments ^{177}Hf$(n,\gamma)^{178}$Hf and ^{177}Hf$(n,\gamma)^{180}$Hf is the same as all other ^{178}Hf lines. But the ratios on these two lines are quite different from each other and from a ^{178}Hf line. Since the 1231.5 keV line intensity increases much more in the ^{180}Hf case and since it is observed in radioactive decay work, at least part of it is from ^{180}Hf.

[c] This intensity is deduced by comparing the triplet envelope of this data to the doublet envelope in the bcs data which contains no carbon line. The bcs establishes the correct ratio for the 1261 and 1249 keV lines. The right amount of of carbon intensity is peeled off from the envelope to establish the 1261 keV line intensity that then gives the proper intensity ratio with the 1249 keV line. The centroid of this single envelope is used to calculate the final energy of 1260.8 keV.

corded with a Ge(Li) detector located inside a split-ring NaI detector.[23] The system was used in the triple coincidence mode [Ge(Li) detector plus the two annilation γ rays detected in opposite quarters of the split-ring NaI detector] which strongly enhances the double escape peak over the full energy peak and the other partial energy loss peaks. The γ-ray energies and intensities are listed in Table IV.

The γ-ray energies were calibrated by comparing them with well calibrated lines in nitrogen,[29] boron,[30] and carbon.[31] The energy values used for these lines are listed in Table V. The relative γ intensities were obtained by comparing the observed intensities with those measured for the ^{15}N calibration lines under similar conditions. This intensity calibration run was in good agreement with previous calibration runs, so a previously established efficiency curve was used to extend the intensity measurements down to 4.7 MeV. Isotopic assignments were made for the γ lines in a similar manner as that described in Sec. II B.

Thermal neutron capture (s-wave neutrons) in the ^{179}Hf sample (ground state $J = \frac{9}{2}^+$) can generate capture states with $J = 4^+$ and 5^+. Dipole primary γ transitions from these states can feed final states with spin $J = 3, 4, 5$, and 6. However, the thermal neutron capture in ^{179}Hf is dominated by capture in a few low-lying 4^+ states, so most of the primary γ strength feeds final states with $J = 3, 4$, and 5. This lack of any appreciable neutron capture in 5^+ states accounts for the extremely weak feeding of the 6^+ state at 640.85 keV. One would not expect to observe a primary transition to a 6^- state for the same reason. In the average resonance neutron-capture runs discussed in the next section (II C), neutron capture proceeds equally to 4^+ and 5^+ capture states so primary γ transitions to 6^+ and 6^- states should be observed. In some cases this difference between thermal neutron capture and average resonance neutron capture can be used to suggest unique spin assignments.

D. Average resonance neutron-capture spectrum

An average resonance neutron-capture γ-ray spectrum[24] was recorded for the ^{179}Hf$(\bar{n},\gamma)^{180}$Hf reaction using the same Ge(Li) detector system described in Sec. II C. A triple coincidence between the Ge(Li) detector and opposite quarters of the split-ring NaI detector was used to enhance the double escape peaks as before and the isotopic assignment was again made by comparing this run with similar average resonance neutron-capture runs using a natural hafnium sample and one enriched in ^{177}Hf. The isotopic abundances of these samples are listed in Table VI. The energy and intensity calibrations were made in

the same way as described in the previous section (II). The γ-ray energies and intensities assigned to the reaction $^{179}Hf(\bar{n},\gamma)^{180}Hf$ are listed in Table VII. The relative intensities have been normalized so that the I_γ for the strong line at 7079.5 keV is equal to 1000. The average neutron-capture process is often denoted by $(\bar{n},\gamma)$ in the rest of this paper.

The average resonance neutron-capture sample consisted of 1.2 g of HfO powder (enriched to 53.835% ^{179}Hf) compressed into a cyclindrical pellet 9.5 mm in diameter and 9.5 mm long. The HfO pellet was surrounded by 1.6 mm layer of ^{10}B powder and incased in a carbon holder. The sample was positioned in the high flux region of the Argonne CP-5 research reactor (see Fig. 9). Figure 10 shows the pulse height spectrum for one of the average resonance capture runs. The peaks labeled with spin and parity assignments are assigned to the $^{179}Hf(n,\gamma)^{180}Hf$ reaction. The peaks from other $(\bar{n},\gamma)$ reactions are labeled with the final nucleus produced in the reaction; thus the label ^{178}Hf refers to the $^{177}Hf(n,\gamma)^{178}Hf$ reaction, ^{13}C to $^{12}C(n,\gamma)^{13}C$, etc.

The 1.6 mm thick layer of ^{10}B absorbs virtually all of the incident thermal neutron flux. The neutrons that reach the ^{179}Hf sample have energies greater than 50 eV. The observed (n,γ) spectrum

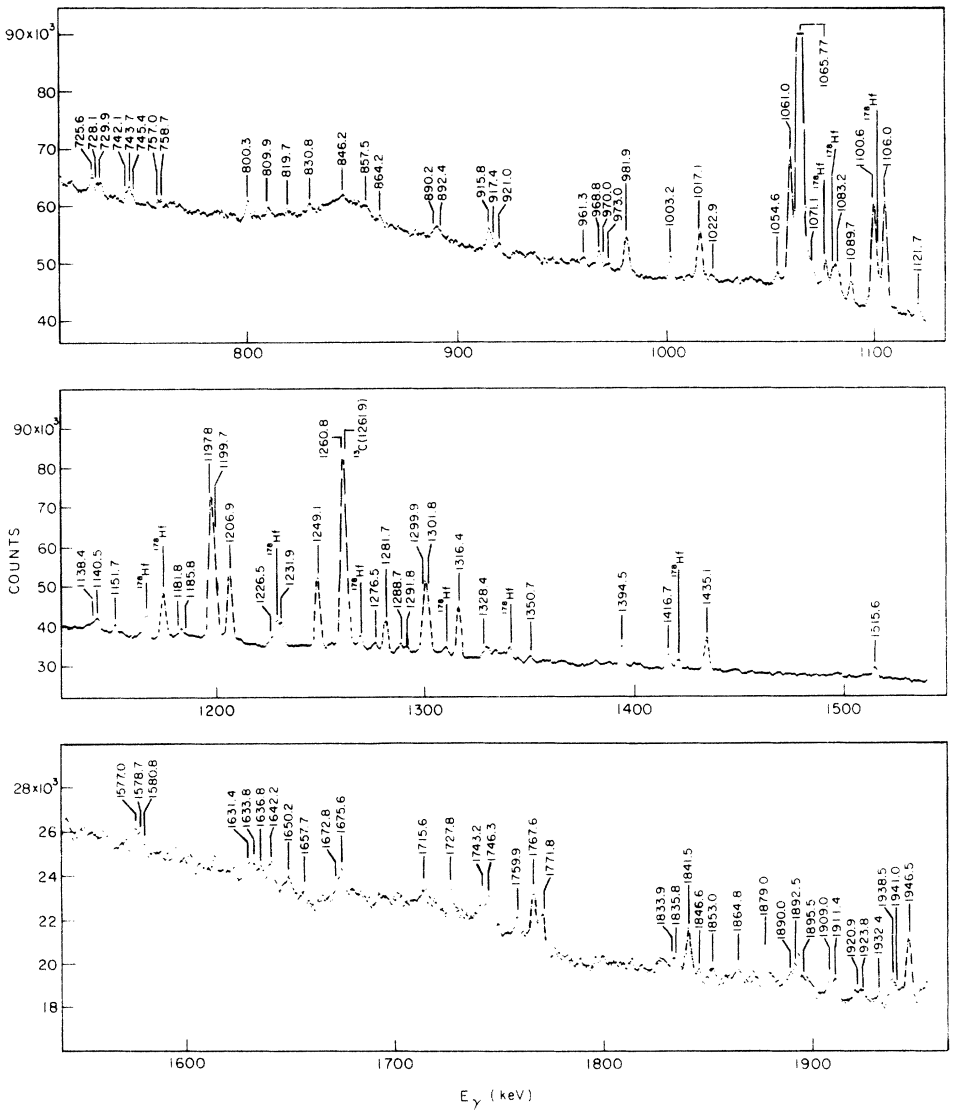

FIG. 8. Medium energy γ-ray spectrum following thermal neutron capture in ^{179}Hf. The Ge(Li) spectrometer employs anticoincidence suppression of all but full energy peaks. The γ rays of measurable intensity are all assumed to be members of cascades. The target for this spectrum has an 83.6% enrichment in ^{179}Hf.

is therefore an average of the (n,γ) spectra from all the neutron-capture resonances above 50 eV and below 10 keV where the incident flux becomes quite low. This averaging reduces the Porter-Thomas fluctuations in the γ intensities that one would expect for neutron capture in a single resonance and makes it possible to determine the multipolarity of a primary γ transition from the relative value of its γ intensity. This multipole identification with relative intensity can be seen most easily in Fig. 11 which is a plot of $\log_{10}[I_\gamma \times (E_1/E_\gamma)^6]$ versus E_γ. The multiplication of I_γ by $(E_1/E_\gamma)^6$ removes the dependence of the relative γ intensity on the γ-ray energy. The sixth power was chosen for the energy dependence because it gave the most constant values for the reduced $M1$ radiation strengths. The use of the fifth power or the seventh power for the energy dependence would give almost as good a fit to a horizontal line and is not ruled out by the data. The $E1$ and $M1$ groups are quite well separated in Fig. 11 which makes the assignment of multipoles to the primary γ transitions a quite straightforward process. The $E2$ group intensity (dashed horizontal

TABLE IV. Primary γ-ray transitions following thermal neutron capture in ^{179}Hf. E_γ is the primary γ-ray energy as measured with a Ge(Li) detector. E_0 is the capture state energy including the recoil energy, E_R, and has the value 7387.7 ± 0.3 keV. The energies listed in parentheses are of uncertain origin.

E_γ (keV)	Relative intensity	$[E_0 - (E_\gamma + E_R)]$ (keV)	Level energy via avg. resonance $(\bar{n},\gamma)$ (keV)	Remarks
			93.1	
7079.3 ± 0.3	194	308.3	308.6	
6747.0 ± 0.7	24	640.6	640.9	
6192.1 ± 0.6	13	1195.5	1192.4	
			1198.9	
			1260.5	
6096.6 ± 0.4	64	1291.0	1290.9	
6018.8 ± 0.4	140	1369.6	1369.3	
6013.0 ± 0.4	110	1374.6	1374.1	
			1380.9	
5978.8 ± 0.4	95	1409.6	1409.4	
5956.9 ± 0.3	290	1430.8	1430.5	
			1472.5	
5904.6 ± 0.3	80	1483.1	1482.6	
			1484.9	
5847.4 ± 0.2	1000	1540.3	1539.7	
5830.4 ± 0.6	30	1557.3	1557.7	
5778.1 ± 0.4	1050	1609.6	1608.9	Doublet struc ure
5774.5 ± 0.4	390	1613.4	1612.3	
5751.3 ± 0.7	22	1636.4	1637.3	
			1701.0	
5677.8 ± 0.3	310	1709.9	1709.6	
5663.0 ± 0.7	25	1724.7	1724.1	
5572.4 ± 0.4	1490	1815.3	1813.6	Doublet with ^{178}Hf line
			1818.2	
5477.9 ± 0.3	440	1909.8	1910.5	
5353.3 ± 0.4	140	2034.4	2034.8	
5234.4 ± 0.4	550	2153.3	2152.7	
(5074.5 ± 0.6)	150	2313.2		Triplet structure
5071.1 ± 0.4	580	2316.6	2314.5	$(\bar{n},\gamma)$ analysis stops here
5066.6 ± 0.5	150	2321.1		
4910.6 ± 0.5	990	2477.1		
4852.7 ± 0.5	450	2535.0		
4827.2 ± 0.6	350	2560.5		
4748.5 ± 0.6	240	2639.2		
4738.3 ± 0.5	280	2649.4		
4707.8 ± 0.5	1120	2679.9		

TABLE V. Calibration lines for primary transitions in $^{179}Hf(\bar{n},\gamma)^{180}Hf$.

γ-ray energy	I_γ [a] γ's/100n	Capturing isotope	Reference for E_γ
7299.0 ±0.5	10.0	^{15}N	Greenwood (Ref. 29)
7006.3 ±0.3		^{11}B	Thomas (Ref. 30)
6322.0 ±0.4	18.8	^{15}N	Greenwood (Ref. 29)
5533.20±0.35	19.7	^{15}N	Greenwood (Ref. 29)
5269.20±0.35	29.1	^{15}N	Greenwood (Ref. 29)
4945.46±0.17		^{13}C	Prestwich (Ref. 31)

[a] Reference 29.

TABLE VI. Isotopic abundances of hafnium samples used in the average resonance neutron capture experiments.

A	Natural (%)	^{177}Hf enriched (%)	^{179}Hf enriched (%)
174	0.18	<0.10	<0.05
176	5.15	0.76±0.05	0.53±0.05
177	18.39	91.67±0.10	3.01±0.05
178	27.08	4.85±0.10	8.75±0.05
179	13.78	0.92±0.05	57.83±0.10
180	35.44	1.80±0.10	29.89±0.10

TABLE VII. Primary γ rays from ^{180}Hf following average resonance neutron capture in ^{179}Hf. All listed values were obtained from spectra taken with a Ge(Li) detector. E_γ is the primary γ-ray energy. $E_1 = 7079.4$ keV is used as a standard for normalizing the relative intensity, I_γ. E_0 is the capture state energy and is determined by $E_0 = E_1 + 308.58$ keV $+ E_r$ where E_r is the recoil energy. This gives $E_0 = 7388.15 \pm 0.40$ keV. The asterisk on $[E_0 - (E_\gamma + E_R)]$ in column 6 means that due to p-wave capture the energy difference has been corrected for energy shifts between multipoles. For $E1$ radiation the E_0 is reduced by 0.79 keV and for lines made up of $E2$ (s-wave) plus $E1$ (p-wave) radiations it is increased by 0.69 keV. The capture state uncertainty of ±0.4 keV includes calibration error, whereas the errors listed in column 1 are of statistical origin only.

E_γ (keV)	I_γ	$I_\gamma\left(\frac{E_1}{E_\gamma}\right)^6$	$\frac{\Delta I}{I}\times 100$	Multipole	$[E_0-(E_\gamma+E_R)]$* (keV)	Remarks
7295.6±0.4	155	131	30	$E2$	93.1±0.5	
7079.4±0.2	1000	1000	5	$M1$	308.6±0.4	
6747.1±0.3	413	555	15	$M1$	640.9±0.5	
6196.3±0.5	77	173	40	$E2$	1192.4±0.6	
6189.8±0.5	61	138	40	$E2$	1198.9±0.6	
6128.2±0.8	72	171	50	$E2$	1260.5±0.9	
6097.2±0.5	302	757	15	$M1$	1290.9±0.6	
6088.1±0.7	76	190	40	$E2$	1300.6±0.8	
6018.9±0.3	365	955	15	$M1$	1369.3±0.5	
6013.1±0.2	1900	4996	3	$E1$	1374.1±0.5	
6007.1±0.6	197	520	20	$M1$	1380.9±0.7	
5978.6±0.4	316	875	15	$M1$	1409.4±0.6	
5956.7±0.2	1261	3531	4	$E1$	1430.5±0.5	
5916.1±0.3	68	200	40	$E2$ ($M1$)	1472.5±0.5	
5904.6±0.2	1808	5423	4	$E1$	1482.6±0.5	
5903.1±0.8	314	942	20	$M1$	1484.9±0.9	
5847.5±0.2	1346	4294	5	$E1$	1539.7±0.5	
5830.4±0.2	339	1099	15	$M1$	1557.6±0.5	
5791.9±0.8	123	408	35	$M1$	1596.1±0.9	
5778.4±0.4	2290	7770	35	$E1$	1608.9±0.6	Multiplet read as doublet may contain transitions to 1607.6 and 1616 keV +parity states.
5775.0±0.4	2290	7770	35	$E1$	1612.3±0.6	
5751.4±0.6	100	347	35	$M1$ ($E2$)	1637.3±0.7	
5687.0±0.5	186	693	30	$M1$	1701.0±0.6	
5677.7±0.2	1939	7311	10	$E1$	1709.6±0.5	Doublet with ^{179}Hf line at 5673.3 keV
5664.0±1.0	62	236	50	($E2$)	1724.8±1.1	Possible transition in ^{180}Hf
5573.7±0.7	1380	5890	10	$E1$	1813.7±0.8	
5569.0±0.5	1270	5410	10	$E1$	1818.3±0.6	
5477.5±1.7	340	1585	20	$M1$	1910.6±1.8	
5353.2±1.3	357	1910	20	$M1$	2034.9±1.4	
5235.3±0.8	1430	8850	10	$E1$	2152.0±0.9	
5072.8±0.8	1130	8380	10	$E1$	2314.6±0.9	

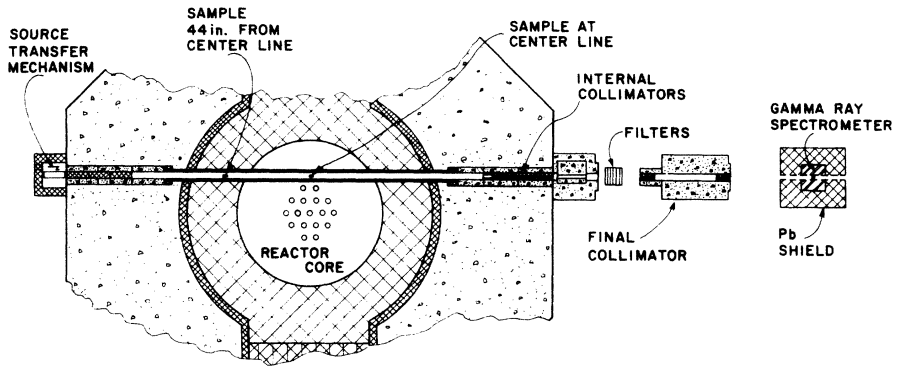

FIG. 9. Schematic drawing of the layout of the germanium detector facility at the Argonne CP-5 research reactor.

line in Fig. 11) is arbitrarily set equal to the intensity of the primary γ transition to the first 2^+ state in ^{180}Hf. This γ intensity is partly made up of $E1$ radiation that follows p-wave neutron capture, so the $E2$ label is put is parenthesis. The $E1$ and $M1$ multipole groups are each divided into two subgroups corresponding to primary transitions to final states with $J=4$ or 5 and $J=3$ or 6. The $J=4$ or 5 subgroup is about twice as strong as the $J=3$ or 6 group. This is expected since there are twice as many ways to feed a $J=4$ or 5 state as there are to feed a $J=3$ or 6 state. The different modes of feeding final states with primary γ transitions from s-wave and p-wave neutron capture are illustrated in Fig. 12. The $M1$ intensities also contain an $E1$ component related to p-wave

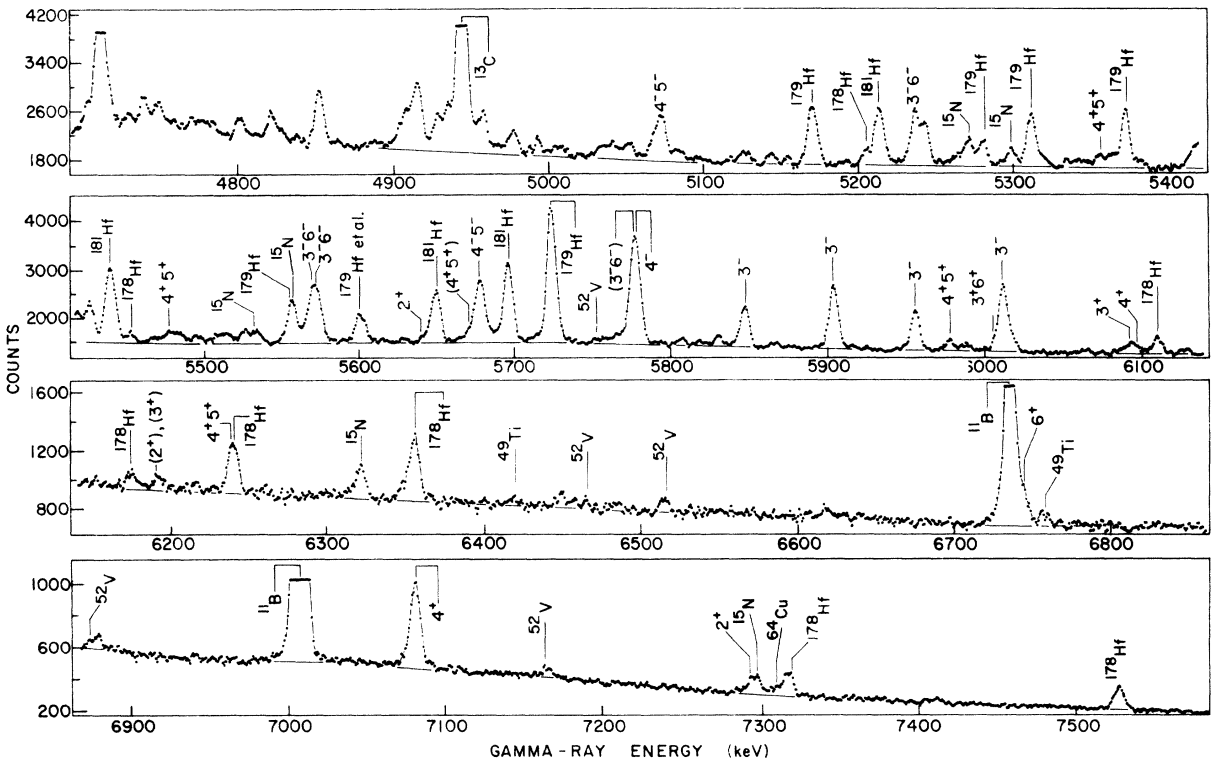

FIG. 10. Spectrum of the primary γ-ray transitions following average resonance neutron capture in a target enriched to 57.8% in ^{179}Hf. Lines from transitions in ^{180}Hf are depicted by a J^π value. Similar spectra from two other targets, one of natural abundance and one enriched to 91.7% in ^{177}Hf, were used for comparison to identify isotopic origins of the spectral lines.

neutron capture as well as an $E2$ component. The ratio of $E1$ strength to $M1$ strength is therefore slightly larger than the ratio read directly from the graph.

In the development of the level scheme in Sec. III, the multipolarity of the primary γ transition will be used to assign a parity to the corresponding final state and to limit the choice of possible spin assignments. When it is possible to identify the transition with one of the multipole subgroups, this limits the spin to two values and becomes a very powerful tool for determining spin assignments.

III. LEVEL SCHEME OF ^{180}Hf

The (n, γ) results reported in this paper were combined with previously published information to construct the level scheme of ^{180}Hf. This level scheme and the details of the γ transitions con-

TABLE VIII. Levels in ^{180}Hf. The level energies and the spin and parity assignments based on average resonance neutron capture $(\bar{n}, \gamma)$ only are listed in the first two columns. The energies and assignments given in the level scheme and based on all data including $(\bar{n}, \gamma)$ are listed in columns 3 and 4.

$(\bar{n}, \gamma)$ results		Final level energies	Final spin and parity
E_{level} (keV)	J^π	(keV)	J^π
93.1	2^+	93.324 ± 0.002	2^+
308.6	4^+	308.576 ± 0.003	4^+
640.9	6^+	640.85 ± 0.01	6^+
		1083.94 ± 0.05	8^+
		1107.2	0^+
		1141.49 ± 0.06 [a]	8^-
		1164.2	0^+
1192.4	3^+6^+	1192.6	6^+
1198.9	2^+7^+	1199.7	2^+
1260.5	2^+7^+	1260.8	2^+
1290.9	4^+5^+	1291.0	4^+
1300.6	2^+7^+	1300.36	2^+
1369.3	4^+5^+	1369.5	4^+
1374.1	3^-6^-	1374.35	3^-
1380.9	3^+6^+	1381.57	3^+
1409.4	4^+5^+	1409.2	4^+
1430.5	3^-6^-	1429.8	3^-
1472.5	$2^+3^+6^+7^+$	1472.3	6^+, (7^+)
1482.6	3^-6^-	1482.66	3^-
1484.9	4^+5^+	1484.6	4^+
1539.7	3^-6^-	1539.3	3^-
1557.6	4^+5^+	1559.28	4^+
1596.1	$2^+3^+6^+7^+$	1597.4	(3^+), 6^+
		1607.63	3^+, (4^+)
1608.9	$3^-4^-5^-6^-$	1609.4	3^-
1612.3	$3^-4^-5^-6^-$	1612.97	4^-, (5^-)
1637.5	$2^+3^+6^+7^+$	1637.1	2^+
1701.0	4^+5^+	1700.8	5^+

[a] 5.5 h isometric state.

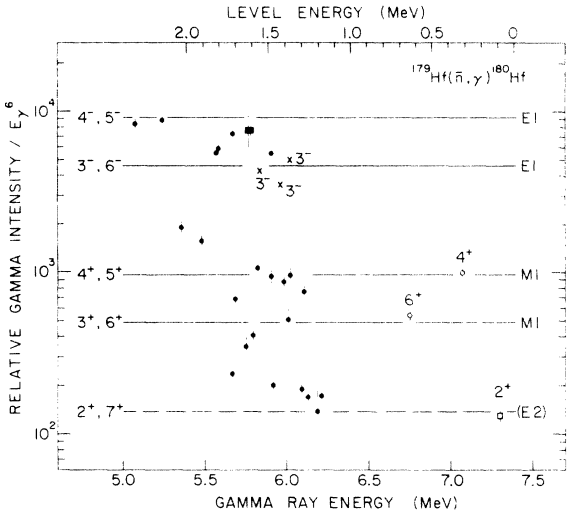

FIG. 11. The intensities of primary γ rays following average resonance neutron capture in ^{179}Hf as a function of energy. An E_γ^6 energy dependence is removed from the intensity to obtain an approximate equalization of all transition intensities of a particular multipolarity. The pair of straight lines for each of the $E1$ and $M1$ intensity levels are drawn with a separation corresponding to an intensity ratio of 2 as suggested by the selection rules. The known 3^- states are located with ×'s. The known $M1$ and $(E2)$ transitions are indicated by open circles and squares, respectively.

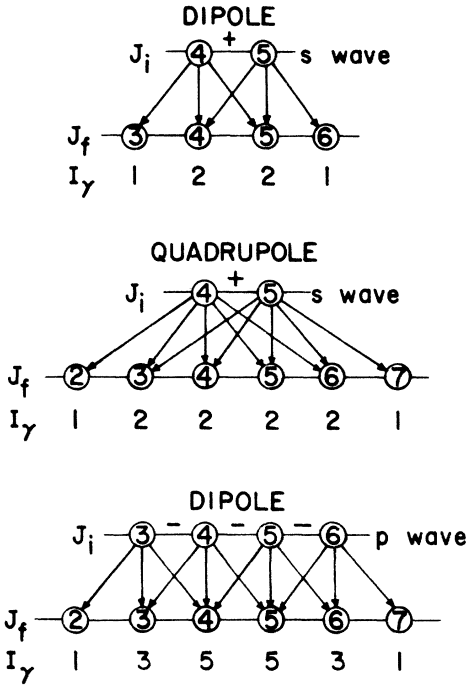

FIG. 12. Schematic representations of the different modes of feeding final states with primary γ transitions following both s-wave and p-wave neutron capture into the $\frac{9}{2}^+$ ground state of ^{179}Hf.

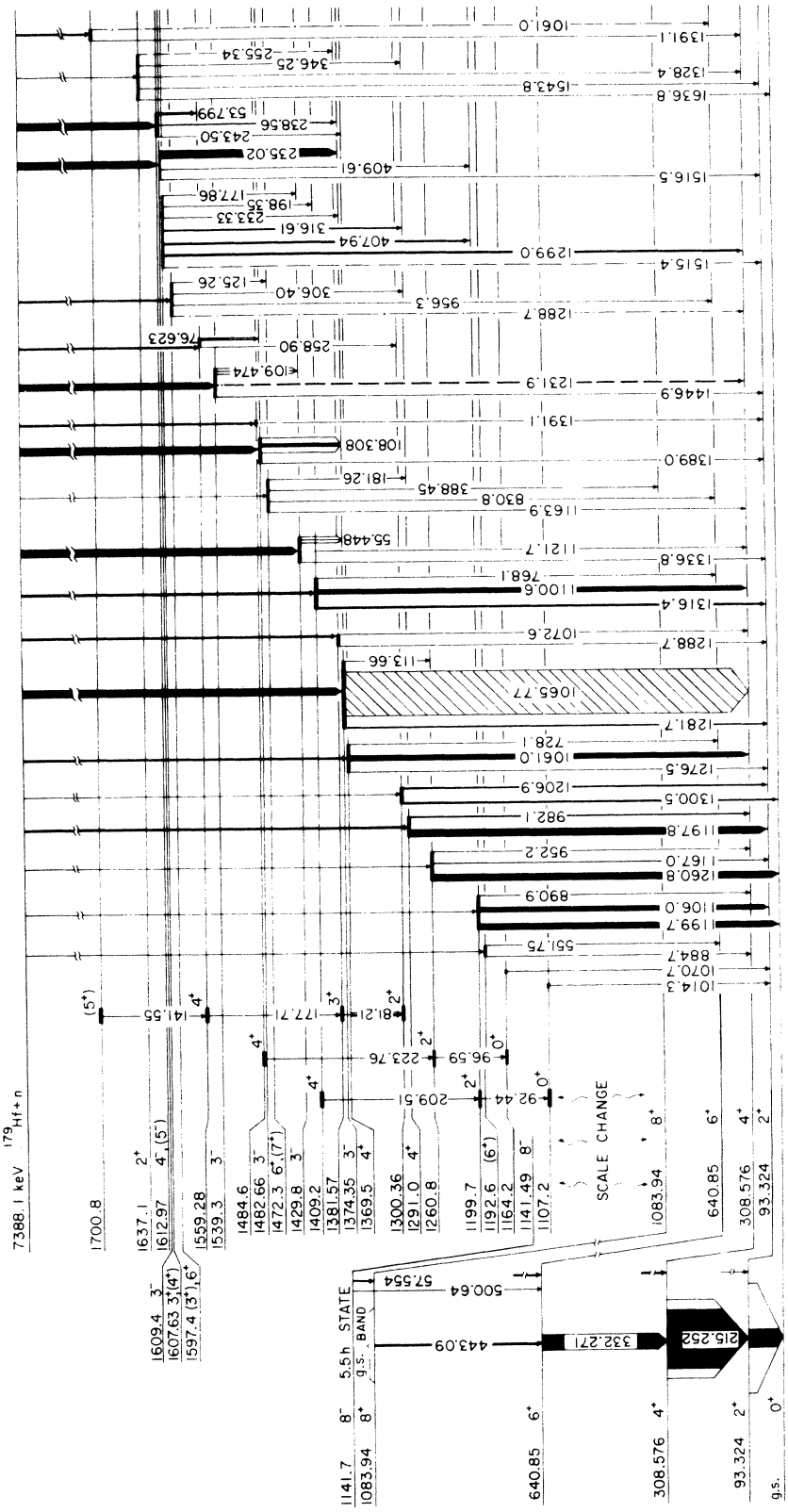

FIG. 13. The level scheme of ^{180}Hf up to 1700.8 keV as deduced from neutron capture γ-ray measurements. A transition with long dashes indicates that the energy fit is not within listed errors. A dot-dash transition indicates that this is a second placement and that the other placement is more certain. The ground state rotational band is shown at the left scaled up for detail. Average resonance primary transitions from the capture state to an energy level are drawn having three different widths—the thickest corresponds to $E1$ radiation, the next size narrower corresponds to $M1$ radiation, while a thin line corresponds to $E2$ radiation. A parenthesis around a single J^{π} assignment indicates that the assignment is tentative. If a parenthesis is placed around one of two listed choices it signifies that the choice is not ruled out but is less likely than the other choice.

TABLE IX. Levels in ^{180}Hf above 1700 keV. In column 3 the level energy as predicted by primary transitions from average capture $(\bar{n},\gamma)$ and thermal capture are listed respectively where available. The multipolarity of the $(\bar{n},\gamma)$ primary transition is given in column 4. Transitions to final states are described in columns 5 to 8.

Initial state		E_0-E_γ $(\bar{n},\gamma)$ (n,γ)		Final state		Transition	
E_{level} (keV)	J^π	(keV)	Multipole	E_{level} (keV)	J^π	E_γ (keV)	I_γ (photons per 100 captures)
1709.1	4^-, (5^-)	1709.6 1710.1	$E1$	308.58	4^+	1400.5 ±0.5	0.16
1724.7	2^+, 3^+	1724.8	$E2$ or $M1$	93.324	2^+	1631.4 ±0.7	0.12 [a]
		1724.9		308.58	4^+	1416.7 ±0.3	0.51
				1291.0	4^+	433.71 ±0.12	0.34
				1369.5	4^+	355.20 ±0.10	0.1
1743.4	2^+			g.s.	0^+	1743.2 ±0.2	0.21
				93.324	2^+	1650.2 ±0.7	0.14
				1291.0	4^+	452.53 ±0.16	0.16
				1429.8	3^-	313.50 ±0.10	0.13
				1484.6	4^+	258.90 ±0.03	0.10 [b]
1813.9	3^-	1813.6	$E1$	93.324	2^+	1721.0 ±0.7	0.07
		1815.5		1539.3	3^-	274.6 ±0.1	0.16
				1559.3	4^+	254.6 ±0.9	0.19
1818.5	3^-, 6^-	1812.2	$E1$	308.58	4^+	1510.5 ±0.7	0.11
				1612.97	4^-5^-	205.51 ±0.01	1.35
1909.7	4^+, 5^+	1910.5	$M1$	1199.7	2^+	709.8 ±0.4	0.16
		1910.0		1607.63	3^+4^+	302.06 ±0.8	
1945.3	2^+			g.s.	0^+	1946.5 ±0.7	0.44 [a]
				93.324	2^+	1853.0 ±0.7	0.08 [a]
				308.58	4^+	1636.8 ±0.5	0.14 [b]
				1199.7	2^+	745.4 ±0.4	0.14
				1291.0	4^+	654.9 ±0.6	0.13
				1559.28	4^+	385.84 ±0.14	0.19
2034.4	4^+5^+	2034.8	$M1$	93.324	2^+	1941.0 ±0.7	0.1
		2034.6		1291.0	4^+	743.4 ±0.2	0.24
				1482.66	3^-	551.75 ±0.06	0.24 [b]
2151.6	3^-, (4^-)	2151.9	$E1$	93.324	2^+	2058.3 ±1.7	0.1
		(2153.5)		1199.7	2^+	953.2 ±0.7	0.05
				1260.8	2^+	890.9 ±0.4	0.28
				1612.97	4^-, 5^-	538.39 ±0.04	0.65
2316.6	(4^-), 5^-	2314.5	$E1$	308.58	4^+	2008.3 ±1.7	0.15
		2316.8		1609.4	3^-	707.3 ±0.5	0.09
				1612.97	4^-, 5^-	703.3 ±0.5	0.11
				2034.4		282.28 ±0.08	0.42
2476.9	5^-			640.85	6^+	1835.8 ±1.0	0.07
		2477.3		1291.0	4^+	1185.8 ±0.6	0.12
				1409.2	4^+	(1066 ±)	
				1539.3	3^-	937.8 ±0.5	0.16
				1559.28	4^+	917.4 ±0.5	0.25
				1612.97	4^-, 5^-	864.2 ±0.3	0.14
				2316.6	5^-	160.4 ±0.03	0.12
2680.0	$4^\pm$, 5^-			1192.6	6^+	1488.0 ±1.0	0.06
		2680.1		1539.3	3^-	1140.8 ±0.8	
				1612.97	4^-, 5^-	(1066 ±) [c]	
				1700.8	5^+	979.2 ±0.7	0.11
				2316.6	5^-	363.32 ±0.10	0.16

[a] Energy fit not within errors.

[b] Has been placed in level scheme below 1700 keV.

[c] A possible alternative placement for some portion of the 1065.77 keV γ-ray intensity.

necting the individual levels are presented in Fig. 13 and Table IX. All of the level energies, γ-ray energies, and γ intensities presented in the level scheme are based on the (n,γ) work presented in this paper. Most of the spin and parity assignments are also based on the (n,γ) work but whenever possible, corraborative evidence from other experiments is used as well. The energy of the level, in keV, is given on the left followed by the spin and parity assignments. The shaded width of the γ transitions is proportional to their measured γ intensity. The unshaded width of the γ transitions is proportional to conversion electron intensity. The width of the solid arrows above the γ decay group for a level is meant to suggest the reduced γ intensity of the primary transition that feeds this level in the average resonance neutron-capture experiment. The thickest lines correspond to strong $E1$ transitions to negative parity states, the intermediate thickness lines to $M1$ transitions to positive parity states, and thinnest lines to $(E2)$ transition positive parity states. The dash is used for transitions when their placement in the level scheme is uncertain and a dot dash for a possible transition which is definitely located elsewhere but which satisfies energy and selection rule requirements. Three prospective rotational bands are described near the left side of Fig. 13.

Before undertaking a detailed discussion of the characteristics of the level scheme, it is important to make a few general observations. In the first place, the medium-energy γ-ray spectrum is quite complicated—especially in the region from 500 to 1000 keV. In this energy region there appear a large number of weak γ rays whose intensities are at or just above the limit of sensitivity. Associated with this fact is the existence of many weak multiple line structures and concomitant background uncertainties. We have not been able to separate out the component lines in many of these structures by the standard methods. This spectral complexity makes it more difficult to rule out transitions or to sot low upper limits to the intensity of a possible transition since the probability is high that a prospective line, predicted because of the level scheme, can be found in the spectrum having the correct energy within limits set by statistical errors.

Secondly, the average level density in the energy range studied for this level scheme is quite high and the number of transitions is so large that there appear to be virtually no transition restrictions characteristic of interband forbiddance. The normal selection rules for multipole radiation seem to predominate.

Thirdly, because of the probability of accidental fits, statistical criteria had to be adopted in order to avoid rather arbitrary rejections of good energy fits. This problem becomes increasingly significant above 1600 keV, where transitions from a given initial state go to more and more final states whose spin assignments are indefinite.

In the first section of the level scheme (Fig. 13) we have avoided this problem of accidental fits wherever possible by utilizing the results of the γ-γ coincidence measurements of Gujrathi and D'Auria.[21] Also, the level density is appreciably less in the lower regions of the level scheme and the spin assignments are more certain; thus the placement of γ-ray transitions in Fig. 13 is believed to be quite reliable. A continuation of the level scheme to 2680 keV is presented in tabular form (Table IX) rather than a figure since the increasing probability of accidental fits makes the over-all description appreciably less reliable. In some cases the chance of an accidental fit in this higher-energy region is as high as 35%. As the uncertainty in the placement of low-energy γ rays increases the chance of inferring anything about the relative spins of two levels because they are connected by a γ transition decreases. In trying to choose between a 3^- assignment and a 6^- assignment in Table IX a single transition to a 2^+ or 3^+ or 4^+ state is not sufficient. One needs at least two transitions to 2^+, 3^+, and 4^+ states to make a meaningful choice. Each level in the level scheme development was treated separately, but in no case was a spin and parity assignment made solely on the basis of the existence of a few low-energy γ transitions. In a few cases accidental fits were ruled out when they conflicted with well determined spin and parity assignments for the initial and final states.

The placement of the 1065.77 keV γ ray led to some complications in the level scheme. We have concluded that most of the intensity of this very intense line ($I_\gamma = 23.7$ photons per 100 n captures) must be assigned to a γ transition from the 3^- level at 1374 keV to the 4^+ level 308.576 keV. Gujrathi and D'Auria[21] saw a strong 1066 keV line in their spectrum and have placed its total intensity in the same place in the level scheme. However, our ratio of the intensity of the 1065.77 keV line to that of the competing 1281.2 keV line to the first 2^+ state (I_γ 1065.77/I_γ 1281.7 = 23/1) is in strong disagreement with the ratio ($\frac{6}{1}$) reported by Gujrathi and D'Auria.[21] It is possible to assign some of the intensity of the 1065.77 keV line (4 photons per 100 n captures) to a γ transition between the levels at 2476.2 and 1409.2 keV, but this only reduces the $I_\gamma 1065.77/I_\gamma 1281.2$ ratio to $\frac{19}{1}$. The error in our ratio is about $\pm 6\%$ while that of Gujrathi and D'Auria might be as large as 40%, but the disagreement still exists even with these

large errors. There seems to be two possible alternatives: either the 1282 keV line in the data of Gujrathi and D'Auria includes another line or an escape peak from a line beyond the end of their spectrum or our 1065.77 keV line is a multiplet consisting of 2 or 3 relatively strong lines one of which is not placed in our level scheme. A third possible placement for a 1066 keV line occurs between the levels at 2679.2 and 1613 keV, but the γ decay of the 1613 keV level is so weak that no appreciable γ strength can be accounted for in this manner. If the 1065.77 keV line is a triplet then it is a very unusual situation because the Ge(Li) detector data does not show even a hint of any line broadening. To check the possibility that the 1065.77 keV line might be a doublet a special experiment using both the bent-crystal spectrometer and a Ge(Li) detector was performed. In this experiment the bent-crystal spectrometer was set at several positions on the 1066 keV diffraction peak and the diffracted γ radiation was examined with the Ge(Li) detector. Normally when a close doublet is examined in this manner[15] the centroid of the peak in the Ge(Li) detector shifts slightly as the diffraction angle is changed. This comes about because a change in the diffraction angle changes the relative amounts of the two components diffracted into the Ge(Li) detector. In this case no shift was observed which strongly suggests that the 1065.77 keV line is a singlet or a very closely spaced doublet. The possibility that it is a very closely spaced triplet seems even less likely.

About $\frac{3}{5}$ of the intensity of this line is accounted for by the three strong transitions to the 3^- state at 1374.35 keV from the negative parity states at 1429.8, 1482.7, and 1609.4 keV. As discussed in the next section the incoming intensity deficit is not unreasonable so one is not required for the sake of intensity balance to locate some of the 1065.77 keV line intensity elsewhere. Yet if one needed to relocate some intensity for other reasons, the outgoing intensity is enough larger than the incoming intensity to make it possible.

A. Ground-state rotational band

The ground-state rotational band is well known from investigations referred to earlier.[1,21,22] Our average resonance neutron-capture and thermal neutron-capture data corroborate the conclusions reached in the earlier work. In particular, we were able to verify the positive parities of the first three excited states, 2^+, 4^+, and 6^+, and show that the spin assignments are consistant with the γ intensities measured in the average resonance neutron-capture work (see data in Fig. 11). The high-precision bent-crystal spectrometer measurements of the low-energy γ rays enable us to assign very accurate excitation energies to the members of the ground-state band. These values follow the rigid rotor energy dependence $E_L = A\,I\,(I+1)$, very closely suggesting a quite stable deformation for the levels in the ground-state band.

The total intensity $(I_\gamma + I_{c.e.})$ of the transitions that feed the ground state (g.s.) (see Fig. 13 and Table IX) is about 71 photons per 100 n captures or about 71% of the capture rate. The missing 29% is assumed to be associated with a large number of γ transitions from undetected low spin states. The general systematics of level schemes in this mass region of the Periodic Table do not usually have this much γ strength in secondary transitions with energies above 3 MeV so some of the missing 29% must be coming from low spin states below 3 keV that we have failed to identify.

The first 2^+ state at 93.3 keV is depopulated by one $E2$ γ ray with a total intensity of 60.7%. The sum of the intensities $(I_\gamma + I_{c.e.})$ for the transitions feeding this level is 58.2%. The in and out balance is much closer for this level than it was for the g.s. This close balance suggests that we have identified most of the levels that give any appreciable feeding to the first 2^+ level.

As mentioned previously the very strong 1065.77 keV line feeds the 4^+ level at 308.576 keV. When the intensity of this very strong line is added to the intensities of the other lines that feed the 308 keV level the sum is slightly over 48% which is appreciably larger than the total intensity of the 215.252 keV line (42%) that depopulates this state. If 4% of the 1065.77 keV lines is placed in the level scheme between the levels at 2476.2 and 1409.4 keV the feeding of the 308.576 keV level is reduced to 44% which matches the outgoing intensity within the errors of the experiment. This approximate matching does not leave any surplus outgoing strength to account for any feeding of this level from states located above 3 MeV.

If we assume that there should be a few percent more intensity depopulating the 4^+ level than populates the level, then there should be more of the 1066 keV transition placed elsewhere. As discussed before, this can be done without making the intensity balance at the 1374 keV level unreasonable.

The intensity balance at the 6^+ state at 640.85 keV is quite reasonable: the total intensity into the level is 5.3%; the total out is 9.3%. This is also true of the 8^+ state at 1083.94 keV where the total intensity feeding the level is 0.9 while the total depopulating the level is 1.7%.

B. Levels between the ground-state band and 1700.8 keV

1. $J^\pi = 0^+$ level at 1107.2 keV

The evidence for this level is the 1014.3 ±0.6 keV γ transition to the first 2^+ state and the 92.44 keV transition from a 2^+ state at 1199.7 keV. The data support the existence of a $K=0$ band having this state for the band head as shown in the level scheme (Fig. 13). The total intensity of the 92.44 keV transition including conversion is 0.09 and that of the 1014.3 keV γ ray is 0.10. The 209.51 keV γ ray has almost the same energy as that predicted by a rigid rotor model (215.7 keV based on 92.44 keV for the first transition in the band). As can be expected, this band shows a deformation about the same as the ground state.

2. $J^\pi = 8^-$ level at 1141.49 ± 0.06 keV

Previous studies[1,24] have shown that the level at 1141.49 keV is an isomeric state with a half-life of 5.5 h and a $J^\pi = 8^-$. The γ-ray spectrum associated with the decay of this isomeric state was studied with the bent-crystal spectrometer when the reactor was shut down. The energies and intensities of the two γ rays that depopulate this level (57.554 keV transition to the 8^+ level at 1083.94 keV and the 500.64 keV transition to the 6^+ level at 640.85 keV) come from this work done with the reactor shut down. Combining the $E1$ γ energy of (57.544 ±0.006) keV with the 8^+ level energy of 1083.94 ±0.05 keV we obtain 1141.49 ±0.06 keV for the level energy. By comparing the relative intensities of these γ rays and 443.088, 332.271, 215.252, and the 93.324 keV γ rays that complete the γ-decay spectrum we find that the 8^+ state is depopulated by the 500.64 keV transition (18 ±2)% of the time and by the 57.554 keV transition (82 ±2)% of the time. This is in good agreement with the value quoted in previous publications.[1] Both the 57.554 and the 500.64 keV transitions have been studied[1,32] extensively in a search for experimental evidence of parity violation in electromagnetic transitions. The high K forbiddeness ($\Delta K = 8$) of these transitions makes them favorable cases for detecting parity violation.

3. $J^\pi = 0^+$ level at 1164.2 keV

This level is proposed as another $K=0$ band head for a band having members at 1484.6 keV (4^+), 1260.8 keV (2^+), and 1164.2 keV (0^+). The rigid rotor prediction for the 4^+ to 2^+ transitions based on a 96.59 keV 2^+ to 0^+ transition is 225.4 keV compared to 223.76 keV for the actual transition (see Fig. 13). We have not located all of the intensity into this level since the only exhaust transition (1070.7 keV) has an intensity of 0.36 which is 3.6 times the total intensity of the 96.59 keV 2^+ to 0^+ transition.

4. $J^\pi = (6^+)$ and 2^+ at 1192.6 and 1199.7 keV levels, respectively

There is a composite line in the average resonance neutron-capture spectrum that may feed both of these levels. This composite line also contains a line from the ^{177}Hf$(n,\gamma)^{178}$Hf reaction. The full intensity of this peak is a little larger than the intensity expected for the weaker $M1$ subgroup. When fitting this multiplet the ^{177}Hf-$(n,\gamma)^{178}$Hf line was removed first; then two peaks were fitted with one of the peak positions held at 6188.4 keV. This value corresponds to the level energy at 1199.7 keV which was derived from the ~1 MeV γ transitions from this level to the 2^+, 4^+, and 6^+ members of the ground-state rotational band. With the one peak position fixed, the location of the other peak position and the determination of the two γ intensities was relatively straightforward. The 1199.7 keV level is fed by an $E2$ transition with a 2^+ or 7^+ assignment, while the 1192.6 keV level seems to be fed by an $M1$ transition consistent with the weaker $M1$ subgroup corresponding to $J^\pi = 3^+$ or 6^+ although an $E2$ transition is not ruled out. The 1199.7 keV level feeds the first 2^+ and 4^+ states and has been assigned $J^\pi = 2^+$ on this basis. The 1192.6 keV level may feed the first 2^+ state, but the required 1099.6 keV line cannot be separated from the strong 1100.6 keV line which is placed elsewhere in the level scheme. The uncertainty about the feeding of the first 2^+ level makes it difficult to choose between the 3^+ and 6^+ assignments. The 551.75 keV transition to the first 6^+ state has an intensity of 0.24 photons/100 neutron captures. In earlier data from the bent crystal there was a suggestion of a doublet at this energy. Recent data which we obtained from the bent-crystal spectrometer run in the autocycle mode indicate that it is a single line. We have used this transition to determine the level energy of 1192.6 keV in agreement with the value obtained from the average capture data (Table VII). If correctly placed, this γ transition would rule out a 3^+ assignment.

Since the statistics of the average capture spectrum do not allow definite distinction between weak $M1$'s and strong $E2$'s, an assignment of 7^+ remains as a possible choice. However, an 884.7 ±0.7 keV transition to the first 4^+ state gives an energy fit within the error and its intensity (0.1%) is reasonable. In addition, we see no evidence for a transition to the 8^- isomeric state. This seems to suggest that an assignment of 6^+ is more likely.

Because of these uncertainties we have placed parentheses about the J^π value in the level scheme (Fig. 13).

The 1199.7 keV level is a candidate for a 2^+ member of a $K=0$ band having an $E2$ transition to the 0^+ band head at 1107.2 keV.

5. $J^\pi = 2^+$ level at 1260.8 ± 0.2 keV

The $E2$ primary transition to this state observed in average resonance neutron capture is mixed with a transition from ^{178}Hf. When unfolded the resulting intensity indicates an $E2$ transition and a $J^\pi = 2^+$ or 7^+. Transitions to the 0^+, 2^+, and 4^+ members of the ground-state band strongly support a 2^+ assignment. This level is a candidate for the 2^+ member of a $K=0$ rotational band decaying to the 0^+ state at 1164.0 keV by way of the 92.44 keV $E2$ transition.

6. $J^\pi = 4^+$ and 2^+ levels at 1291.0 and 1300.35 keV, respectively

The average resonance data indicate a doublet level structure with a smaller intensity for the lower-energy primary γ ray. After fitting a combination of an $E2$ line shape (low-energy side of the doublet) and an $M1$ line shape to the doublet line structure we concluded that the levels are at 1300.6 keV (2^+ or 7^+) and 1290.9 keV (4^+ or 5^+). A possible transition from the 1291 keV level to the ground state based on a 1291.8 ± 0.5 keV γ ray is thus ruled out due to selection rules. As shown in Fig. 13, transitions to first 2^+ and 4^+ states from the 1291 keV level are consistent with a 4^+ assignment. These two transitions carry about 4 times as much intensity as the total input of four γ-ray intensities which means we have failed to locate a considerable amount of input intensity. Gujrathi *et al.*[21] have assigned a J^π of 3^+ to this level, though a J^π of 4^+ would appear to be consistent with their results. The level energy is obtained after establishing the value for the 1607.63 keV level. Then the 316.61 ± 0.06 keV transition gives 1291.0 keV which is consistent within errors with the transition to the first 2^+ and 4^+ states.

Gujrathi *et al.*[21] have reported a 1299.8 keV γ ray which they placed between the 1607.6 keV level and the first 4^+ state. Our data reveal a 1300 keV line which is about 3 times stronger and which we have read as a triplet (see Table III). We therefore observe a transition to the ground state (1300.5 ± 0.4, $I_\gamma = 1.85$) indicating that the J^π choice for this level should be 2^+ rather than 7^+. The other transition which goes to the first 4^+ (1206.9 ± 0.3, $I_\gamma = 1.60$) is consistent with a 2^+ assignment. The intensity into this level, including the 81.21 keV transition, is 1.33 to 1.36 (depending on whether the 81.21 keV γ ray is $E2$ or $M1$) while 3.45 depopulates the level.

This level is proposed as the band head for a $K=2$ rotational band (see Fig. 13) and though the intensities of the interband cascade are reasonable we see some possible level mixing distorting the energy separations away from the rigid rotor predictions.

7. $J^\pi = 4^+$, 3^- and 3^+ levels at 1369.5, 1374.35, and 1381.6 keV, respectively

The thermal neutron capture forms a doublet whose high-energy member is about 25% more intense than the lower one whereas the average resonance process produces a triplet. The weaker member of the thermal (n,γ) doublet is the strongest member of the average resonance $(\bar{n},\gamma)$ triplet (see Tables IV and VII and 6013 keV line in Fig. 10).

The highest-energy member of the $(\bar{n},\gamma)$ triplet is a primary transition to the 1369.5 keV level and is the stronger of the two $M1$ transitions, suggesting a J^π of either 4^+ or 5^+. Based on there being three γ rays having energies 1276.5, 1061.0, and 728.1 keV depopulating this level to the 2^+, 4^+, and 6^+ states of the ground-state band (see Fig. 13) we have selected $J^\pi = 4^+$ for this level.

The level at 1374.35 keV is clearly a negative parity state based on the high intensity of the primary transition (see Figs. 10 and 11). Its intensity falls in the weaker group of $E1$'s, indicating a spin of either 3 or 6. A 1281.7 keV transition to the 2^+ state at 93.324 keV rules out the choice of 6 for the spin. This placement of the 1281.7 keV transition is supported by Gujrathi *et al.*[21] who used coincidence measurements to determine cascades following β decay to levels in ^{180}Hf.

This is an unusual level in view of the excessive intensity (about 24 photons/100 neutrons captured) of the 1065.77 ± 0.08 keV transition (see Tables II and III) which was previously discussed in this paper. The energy of this γ ray has been determined by using the data from both the Ge(Li) spectrum and the bent-crystal spectrum. The Ge(Li) data resolve members of a line which is a doublet in the bent-crystal spectrum having a centroid energy of 1065.60 ± 0.06 keV and provides both an intensity ratio and line separation for unfolding the bent-crystal spectrometer (bcs) doublet. The bent-crystal calibration then gives the energy. This energy plus that of the first 4^+ state (308.576 keV) gives 1374.35 ± 0.08 keV for the level energy.

The rest of the intensity in the average resonance primary triplet suggests another primary $M1$

transition whose intensity places it in the weaker of the two $M1$ groups indicating $J^\pi = 3^+$ or 6^+. The two transitions shown in Fig. 13 depopulating this level (1288.7 ±0.5 and 1072.6 ±0.5 keV) to the first 2^+ and 4^+ states suggests $J^\pi = 3^+$. This level is the second member of the $K = 2$ positive parity band and, as previously mentioned, decays to the 2^+ state at 1300.36 keV by way of the 81.21 keV transitions, making the input intensity to decay intensity ratio about 0.5 which is quite reasonable.

8. $J^\pi = 4^+$ level at 1409.2 ± 0.3 keV

The average resonance capture γ ray primary to this level falls in the stronger $M1$ group suggesting $J^\pi = 4^+$ or 5^+. Transitions to the ground-state band members at 2^+, 4^+, and 6^+ suggest $J^\pi = 4^+$. The 209.51 ±0.07 γ ray with an intensity of 0.04 photons/100 neutron captures seems to make this state the third member of a $K = 0$ rotational band.

9. $J^\pi = 3^-$ level at 1429.8 ± 0.1

The level is determined to be a negative parity state from average resonance neutron capture having spin choices of 3 or 6. Transitions to the first 2^+ and 4^+ states and 55.448 keV transition to the 3^- state at 1374.35 keV indicate a spin of 3. A 109.474 keV transition from the 3^- state at 1539.3 keV supplies the bulk of the decay intensity out of this level. The ratio of the intensity in to the intensity in to the intensity out is 0.7 to 0.9 depending on the transition multipolarities of the 55.44.8 and 109.474 keV transitions.

10. $J^\pi = 6^+$ or 7^+, 3^- and 4^+ at 1472.3, 1482.66 and 1484.6 keV, respectively

The average resonance data (see Fig. 10) reveal a strong line at 5904.6 keV to a negative parity state having spin 3 or 6. The line is a doublet having a positive parity component. The line corresponding to the 1472.3 keV level is resolved from the doublet.

The multipolarity of the primary transition to the 1472.3 keV level is either $M1$ or $E2$ but more likely $M1$ (see Fig. 11). In either case the γ rays depopulating the level suggest a high spin rather than low spin choice, hence 6^+ or 7^+. We have not ruled out 7^+ (indicated by parentheses in the level scheme, Fig. 13), but two transitions (1163.9 and 181.26 keV) would have to be removed from the four shown in Fig. 13 to allow a 7^+ assignment. We have used the 388.45 and 181.26 keV transitions to determine the level energy of 1472.3 ±0.2 keV.

The negative parity state decays via the intense 108.308 keV transition to help supply some of the intensity for the 3^- state at 1374.35 keV. This establishes its energy to be 1482.66 ±0.08 keV and requires the 3^- rather than the 6^- choice for J^π as does the 1389.0 ±0.7 keV transition to the first 2^+ state.

The positive parity component of the primary doublet falls in the 4^+, 5^+ $M1$ group. The level separation from the 1482.66 keV level, as provided by the primary doublet, allows an excellent energy fit for the 223.76 keV transition to the 2^+ state at 1260.8 keV and makes this state an excellent candidate for the 4^+ member of a $K = 0$ rotational band. A transition to the first 2^+ state at 93.324 keV is also observed.

11. $J^\pi = 3^-$ and 4^+ levels at 1539.3 and 1559.28 keV

The average resonance data reveal an $E1$ transition which indicates that $J^\pi = 3^-$ or 6^-. Thermal neutron capture produces an intense primary of the same energy as well. Transitions to the 2^+ level and possible the 4^+ level in the ground-state band require the lower spin. The strong 109.474 keV transition to the 3^- at 1429.8 keV helps to provide a reasonable intensity balance for the latter level and establishes the energy to be 1539.3 ±0.1 keV. Gujrathi *et al.*[21] report a level at 1539.9 keV with the same transitions to the first 2^+ and 4^+ states. However, we differ on the relative intensity of the 1446.6 and 1231.9 keV transitions. Either we should place some of the 1231.5 keV intensity elsewhere or we may have two close lying levels of similar spin. We may be exciting a 3^- state with (n, γ) and a low spin positive parity state, the latter of which is excited by β decay and seen by Gujrathi *et al.*[21]

The 4^+ state at 1559.28 is a candidate for the third member of the $K = 2$ band and is suggested by an $M1$ primary transition observed in the average resonance spectrum. The band transition of 177.71 keV to the 3^+ state and the 76.623 keV γ ray to the 3^- level at 1482.66 keV give an energy of 1559.28 keV. The crossover transition (258.90 keV) to the 2^+ band head is in agreement with this value. Transitions to the ground-state band are missing. The level energy does not agree too well with the values obtained from the primaries from $(\bar{n}, \gamma)$ or (n, γ), which are about 1.5 keV lower. If this lower energy level also existed, a strong 1249.1 keV transition to the 4^+ state of the ground-state band and a weaker 917.4 keV γ transition to the 6^+ member would then be possible.

We have not included the level reported by Gujrathi *et al.*[21] at 1527 keV since our strongest evidence for it is the existence of a 1435 keV γ ray in our spectra which may correspond to their reported 1434.3 keV γ ray. Comparison

of runs using different targets has shown that its relative intensity when compared with known ^{180}Hf lines changes considerably. There may be some intensity in it due to ^{180}Hf but we have no evidence to verify this. In addition we have not observed the 1219.2 keV γ ray which Gujrathi *et al.*[21] place at this level.

12. $J^\pi = (3^+)$, 6^+ level at 1597.4 keV

The higher spin for this level seems to be more likely since the lowest spin state to which the level decays is 4 and there are energy fits for transitions to 6^+ states.

13. $J^\pi = 3^+$, (4^+) and 3^-, (6^-) and 4^- levels at 1607.63, 1609.4, and 1613.0 keV, respectively

The average resonance neutron-capture γ-ray spectrum reveals a widened line at 5778 keV with sufficient intensity to account for two $E1$ transitions to two negative parity states and possibly one or two $M1$ transitions as well. The thermal neutron-capture spectrum also reveals two strong transitions forming a close doublet but not surprisingly the doublet shape is somewhat different than the corresponding multiplet in the average capture case. The results of our analysis of the average resonance multiplet under the assumption that it is a doublet is given in Table VII and the results for the thermal capture case is given in Table IV.

Our efforts to obtain a definitive intensity ratio for the two lines associated with the two negative parity states have not succeeded. We have therefore listed an equal intensity case in Table VII (see also Fig. 11). This means that the spin choices for either state are 3, 4, 5, or 6. The transitions depopulating these states suggest that the lower-energy state (1609.4 keV) should have spin 3 but spin 6 is not ruled out and the higher-energy state (1613.0 keV) should have $J = 4$. By using (d,p) excitations Zaitz and Sheline[19] have suggested a 5^- state at about this energy (1610 keV).

In essential agreement with Gujrathi *et al.*[21] we have placed a positive parity state at 1607.63 $\pm$0.02 keV in the level scheme (Fig. 13). The energy is determined as an average of all transitions shown except the 1515.4 $\pm$0.4 keV γ ray which is dashed in the level scheme due to a relatively poor energy fit. The inferiority of this fit may be due to a small systematic calibration shift which we suspect has occurred in the energy region above 1400 keV and which is not reflected in the listed error. The bent-crystal spectrometer data give no evidence for the 69.0 keV transition shown as dashed in the decay scheme of Gujrathi *et al.*[21] The spin assignment is either 3 or 4 with preference for 3.

14. $J^\pi = 2^+$ level at 1637.1 keV

There is a weak $M1$ or an $E2$ primary transition to this state from average neutron capture and a very weak transition observed from thermal capture. We have located four and possibly five transitions to lower levels suggesting a $J^\pi = 2^+$ at 1637.1 keV.

15. $J^\pi = (5^+)$ level at 1700.8 keV

Average capture suggests that there is a $M1$ transition from the capture state belonging to the more intense group and having an energy of 1701 keV. This level is a reasonable candidate as a fourth member ($J^\pi = 5^+$) of a $K = 2$ band decaying to the 4^+ member by way of a 141.55 keV γ ray. Two other possible transitions exist that are consistent with this assignment but the energy fit is relatively poor for the 1061.0 keV γ ray which has been placed at 1369.5 keV level as well.

C. Levels above 1700.8 keV

Summaries of the levels described in Fig. 13 are given in Tables VIII and IX. Since the probability of accidental energy fits of low-energy transitions from the levels in this upper range is greater than for the lower lying levels and since the average resonance neutron-capture spectrum becomes increasingly complicated to analyze, the descriptions of the states above 1700.8 keV are generally less reliable than those shown in Fig. 13. These levels and possible transitions to lower lying states are listed in Table IX. For each of 8 of the 12 levels listed there is an average resonance neutron-capture primary γ ray which helps in deducing the J^π assignments. The existence of the 2^+ states at 1743.4 and 1945.3 keV is based on the transitions to lower lying states. The two states at 2476.9 and 2680.0 keV were observed in the thermal capture primary spectrum, but due to spectral complexity we have not succeeded in analyzing the average resonance data for these two levels. As seen in Table IV there are strong thermal capture lines suggesting these levels. The values of E_L in the first column of Table IX are generally obtained from the transitions to final states. Corresponding level energy estimates from the primary transitions due to average resonance neutron capture and due to thermal neutron capture are listed for comparison in column 3 where the former is listed first and the latter second.

IV. CONCLUSIONS

The fact that we have been able to suggest only three rotational bands other than the ground-state band appears to be due to the complexity of the level scheme. This may be a result of level mixing so that many levels lack a definite character. The behavior of these levels may be dominated by statistical effects rather than some simple form of collective motion.

A recent study of rotational bands in ^{180}Hf by Zaitz and Sheline[19] employing (d,p) transfer reactions suggests some negative parity states whose J^π assignments range from 3^- to 6^- [1371 keV (4^-), 1480 keV (5^-), 1609 keV (5^-), 1689 keV (6^-), 1787 keV (6^-), 1824 keV (3^-), and 1926 keV (4^-)]. Therefore, they should be readily observable using the (n,γ) techniques described in this paper. Assuming that energy differences of a few keV between their level energies and ours are reasonable, we verify the first three states and possibly the sixth but not the states at 1689, 1787, and 1926 keV. It is likely that our levels at 1374.35 keV (3^-), 1482.66 keV (3^-), and 1613 keV [4^-, (5^-)] correspond to their levels at 1371 keV (4^-), 1480 keV (5^-), and 1609 keV (5^-), and it is possible that our level at 1818.5 keV (3^-, 6^-) corresponds to their level at 1824 keV (3^-). Our spin assignments for the 1374.35 and 1482.66 keV states are well supported by the γ-ray connections to other levels so that we are confident that our J^π assignments are correct in these cases. Therefore, we cannot place these levels in the same bands suggested by Zaitz and Sheline.[19]

Since for spin values ranging from 3 to 6 inclusive, we expect to observe all negative parity states, we do not agree with the assignments for the three states at 1689, 1787, and 1926 keV.

ACKNOWLEDGMENTS

The authors wish to thank Georege E. Thomas for supplying a variety of information and assistance with the experimental facilities. Our thanks also goes to Jim Specht for sample preparations, technical assistance, and computer data management.

[1] G. Scharff-Goldhaber and M. McKeown, Phys. Rev. 158, 1105 (1967).
[2] S. B. Burson, K. W. Blair, H. B. Keller, and S. Wexler, Phys. Rev. 83, 62 (1951).
[3] E. der Mateosian and M. Goldhaber, unpublished work reported in Ref. 1. See also M. Goldhaber and R. D. Hill, Rev. Mod. Phys. 24, 179 (1952).
[4] A. Bohr and B. R. Mottelson, Phys. Rev. 90, 717 (1953).
[5] W. F. Edwards, J. W. M. Dumond, and F. Boehm, Nucl. Phys. 26, 670 (1961).
[6] W. F. Edwards and F. Boehm, Phys. Rev. 121, 1499 (1961).
[7] E. Boderstedt, H. J. Kirner, E. Gerdan, J. Radeloff, C. Gunther, and G. Stube, Z. Phys. 165, 57 (1961).
[8] A. C. Li and A. Schwarzschild, Phys. Rev. 129, 2664 (1963).
[9] J. W. Mihelich, G. Scharff-Goldhaber, and M. McKeown, Phys. Rev. 94, A794 (1954); Bull. Am. Phys. Soc. 1, 206 (1956).
[10] A. W. Sunyar, Phys. Rev. 98, 653 (1955).
[11] A. C. Li and A. Schwarzschild, Phys. Rev. 129, 2664 (1963).
[12] R. K. Smither, in *Proceedings of the International Conference on Nuclear Physics with Reactor Neutrons*, edited by F. E. Throw (Argonne National Laboratory Report No. ANL-6797, Argonne, Illinois, 1963), p. 89.
[13] R. K. Smither, in Symposium on Crystal Diffraction of Nuclear Gamma Rays, Athens, Greece, 15–17 June, 1964, edited by Feliz Beohm [Caltech Report, Pasadena, Calif., 1964 (unpublished)], pp. 9–34.
[14] R. K. Smither, in Argonne National Laboratory Report No. ANL-6789 (unpublished), p. 14.
[15] R. K. Smither and A. I. Namenson, Rev. Sci. Instrum. 38, 52 (1967).
[16] R. K. Smither, Phys. Rev. 129, 1691–1708 (1963).
[17] R. K. Smither and D. J. Buss, in *Proceedings of the International Symposium on Neutron Capture Gamma Ray Spectroscopy, Sutdsvik, Sweden, 1969* (International Atomic Energy Agency, Vienna, 1969), pp. 55–63.
[18] A. Namenson, H. E. Jackson, and R. K. Smither, Phys. Rev. 146, 844–852 (1966).
[19] J. I. Zaitz and R. K. Sheline, Phys. Rev. C 6, 506 (1972).
[20] L. Varnell, J. H. Hamilton, and R. L. Robinson, Bull. Am. Phys. Soc. 16, 1156 (1971).
[21] S. C. Gujrathi and J. M. D'Auria, Nucl. Phys. A161, 410 (1971).
[22] D. L. Swindle, T. E. Ward, and P. K. Kuroda, Phys. Rev. C 3, 259 (1971).
[23] G. E. Thomas, D. E. Blatchley, and L. M. Bollinger, Nucl. Instrum. Methods 56, 325 (1967).
[24] L. M. Bollinger and G. E. Thomas, Phys. Rev. C 2, 1951 (1970).
[25] L. M. Bollinger and G. E. Thomas, Phys. Rev. Lett. 18, 1143 (1967).
[26] L. M. Bollinger and G. E. Thomas, Phys. Rev. Lett. 21, 233 (1968).
[27] J. A. Bearden, *X-ray Wavelengths and X-ray Atomic Energy Levels* (U.S. Government Printing Office, Washington, D. C., 1967).
[28] L. V. Groshev *et al.*, Nucl. Data A5, 249 (1969).
[29] R. C. Greenwood, Phys. Lett. 27B, 274 (1968).
[30] G. E. Thomas, private communication.
[31] W. V. Prestwich, R. E. Cote, and G. E. Thomas, Phys. Rev. 161, 1080 (1967).
[32] K. S. Krane, C. E. Olsen, J. R. Sites, and W. A. Steyert, Phys. Rev. C 4, 1906 (1971).